Role of β-catenin and Active Beta Catenin in Osteosarcoma Progression
by

Geetha Venkateswaran

A thesis submitted in partial fulfillment of the requirements for the degree of

Master of Science

Medical Sciences - Pediatrics
University of Alberta

Abstract

Osteosarcoma (OS) is the most common primary bone malignancy with a high incidence in children and adolescents. Current treatment strategies (surgery and adjuvant chemotherapy) has improved the overall survival rate of patients with primary OS. However, the survival rate of patients with metastatic disease still remains poor. Therefore, understanding the biology of OS progression would be of key importance to identify markers with prognostic value and potential therapeutic targets for OS. Deregulation of the Wnt signaling pathway is known to be implicated in OS. However, the role of β-catenin (key regulatory component of Wnt signaling) in this cancer is not clear. While some studies support the involvement of β-catenin in OS, others show the contrary. However, to date studies have investigated the role of β-catenin rather than Active Beta Catenin (ABC), a subpopulation of β-catenin that is transcriptionally active. ABC transcribes the Wnt target genes that are involved in cell proliferation, invasiveness and hence promotes cancer.

This study investigated the role of β-catenin and ABC in OS progression using two pairs of cell lines representing OS progression. Western blot analysis, immunofluorescence analysis and high content analysis were carried out for the determination of cellular level and sub-cellular localization of β-catenin and ABC. Our results suggested an association between ABC and OS progression, whereas the total β-catenin by itself was not associated with OS progression. Hence, this study demonstrated the potential role of ABC in OS progression.

A dedication to my grandfather Mr. K.V.Nageswaran

Acknowledgements

I would like to sincerely thank my supervisor Dr. Sujata Persad for giving me the best graduate experience! She has been a great mentor who understood my interest for research, provided me with various opportunities to learn, and guided me to grow as a researcher. Thank you very much for your guidance and unwavering support.

I reverentially thank my committee members, Dr. David Eisenstat and Dr. Mary Hitt, for their invaluable suggestions during the committee meetings. Beyond the discussion at the meetings, they both have extended their support by helping me carry out various experiments in their laboratories. I thank Dr. Hitt for spending hours together in guiding me to design the Active Beta Catenin construct for the project. I thank Dr. Eisenstat for helping with his laboratory resources to carry out IHC experiments. I would like to express my gratitude to both my committee members for all their support; it has been pivotal to shape this project.

Thanks to Dr. Eugenie Kleinerman, University of Texas, MD Anderson Cancer Center for her kind gift of the cell lines SaOS2 and SaOS2-LM7 that were used in this study.

I would like to thank my lab members, Li Hao, Jenny, Sara, Elizabeth and Sue for being there for me. Special thanks to my summer students Linda Xia, for being a great help in carrying out some replicates for my western blotting experiments and Michael Wollin for helping with IF staining on tissue samples. My hearty thanks to all the members of Baksh lab for always being there to discuss and help me troubleshoot experiments!

My thanks to Dr. Richard Schulz and his lab members for being so welcoming and help me to carry out all the gelatin zymography experiments in their lab. I would like to thank Dr. Sun and Ms. Geraldine Barron in the microscopy facility at the Cross Cancer Institute, for the intensive

training and extensive support to use confocal and high content microscopy. Thanks a million to Mr. Powel Crosley for spending hours together with me to figure out specific method of analysis for my high content microscopy data! I would also like to thank Mr. Hunter Mccoll for teaching me IHC staining and help in carrying out optimizations.

Thanks to the Hair Massacure/Stollery Children's Hospital Foundation for the funding to this project. I also thank the Medical Sciences Graduate Program (MSGP) and Women & Children's Health Research Institute (WCHRI) for the graduate scholarships that supported my stipend.

Last but not the least I would like to profoundly thank my family and friends for their good will and moral support. I am very grateful to your love and support.

Table of Contents

List of abbreviations

ALLN - N-acetyl-Leu-Leu-Norleu-al

AP – Alkaline phosphatases

APC – Adenomatous polyposis coli

Asp – Aspartic acid

BCA - Bicinchoninic acid

BMU – Basic multicellular unit

c-Cbl – Casitas B-lineage lymphoma

CDK4 – Cyclin dependent kinase 4

CIN – Chromosomal instability

CKI – Casein kinase I

CSF-1 – Colony stimulating factor – 1

CT – Computed Tomography

CTD – C-terminal domain

CTGF – Connective tissue growth factor

CXCR4 – C-X-C-chemokine receptor 4

CXCL 12 – C-X-C-chemokine ligand 12

DFS – Disease free survival

Dkk – Dickkopf

DTC – Disseminated tumor cells

Dvl – Dishevelled

E-cad – E-cadherin

Eph – Ephrin

FAK – Focal adhesion kinase

FBS – Fetal bovine serum

FDG – Fluorodeoxyglucose

Fz – Frizzled receptor

Glu – Glutamic acid

GSK 3β – Glycogen synthase kinase 3β

HIF-1 – Hypoxia induced factor-1

HRP – Horseradish peroxidase

IGF – Insulin growth factor

IHC – Immunohistochemistry

IL-10 – Interleukin 10

IF – Immunofluorescence

LDH – Lactate dehydrogenase

Lys – Lysine

MEM – Minimal essential medium

MDM2 – Mouse double minute 2

MDP – Methylene di-phosphonate

MMP – Matrix metalloprotease

MRI – Magnetic Resonance Imaging

MT1-MMP - Membrane type 1 metalloproteinase

NEAA – Non-essential amino acid

NLS – Nuclear localization signal

NTD – N-terminal domain

OPG – Osteoprotegerin

OS – Osteosarcoma or Osteogenic sarcoma

PBS – Phosphate buffered saline

PET – Positron Emission Tomography

PI3K – Phosphoinositol-3-kinase

PTH – Parathyroid hormone

RB – Retinoblastoma

SCF – Skp, cullin, F-box

SFRP - Secreted frizzled related proteins

SV40 – Simian Virus 40

TBS – Tris buffered saline

TGFβ – Transforming growth factor β

TIMP2 - Tissue inhibitor of metalloproteinase

uPA – Urokinase plasminogen activator

VEGF – Vascular endothelial growth factor

WIF - Wnt inhibitory factor

WT – Wild type

List of tables and figures

Chapter 1.0
Introduction

1.0. Introduction

1.1. Anatomy of long bone

Bone is a mineralized connective tissue that continuously adapts through the life of a vertebrate in order to maintain the size and structural integrity. The general structure of a long bone comprises a tubular diaphysis or shaft, forming the long axis of bone, and expanded head at each end called the epiphysis. All long bones have a solid outer shell called the compact bone encasing a central space. At the diaphysis region, the central space is called the medullary cavity which contains the bone marrow, and at the epiphyseal region, the central space is occupied by a loosely organized form of bone, called spongy (cancellous) bone (1, 2). Another feature of long bone is the membranes that line them. The entire outer surface of long bone is covered by a double-layered membrane called periosteum. The outer layer of periosteum is primarily composed of collagen fibers, whereas, the inner (cambium) layer that abuts the bone is highly cellular, comprising mesenchymal progenitor cells (3). On the other hand, the internal surface of the bone is lined with a delicate membrane called endosteum.

The structural unit of compact bone is called an osteon or haversian system, which has concentric layers of matrix arranged around a central canal. Running through these haversian canals are small blood vessels and nerve fibres that serves the needs of osteon. Another type of canal called the perforated or Volkmann's canals lie at right angles to long axis of bone and helps in connecting the periosteal blood vessel to those in central canals and medullary cavity (1, 2).

1.2. Composition of bone

Bone is composed of cellular matter, organic and inorganic material. One third of the bone matrix is composed of organic material called osteoid. Osteoid includes ground substance like proteoglycan, glycoproteins etc., and collagen fibres. The remaining two thirds of bone matrix consists of inorganic hydroxyapatite or calcium phosphate. While the organic material of bone matrix provide resilience, the inorganic mineral salts account for the hardness of bone and resistance to compression (2).

A) B)

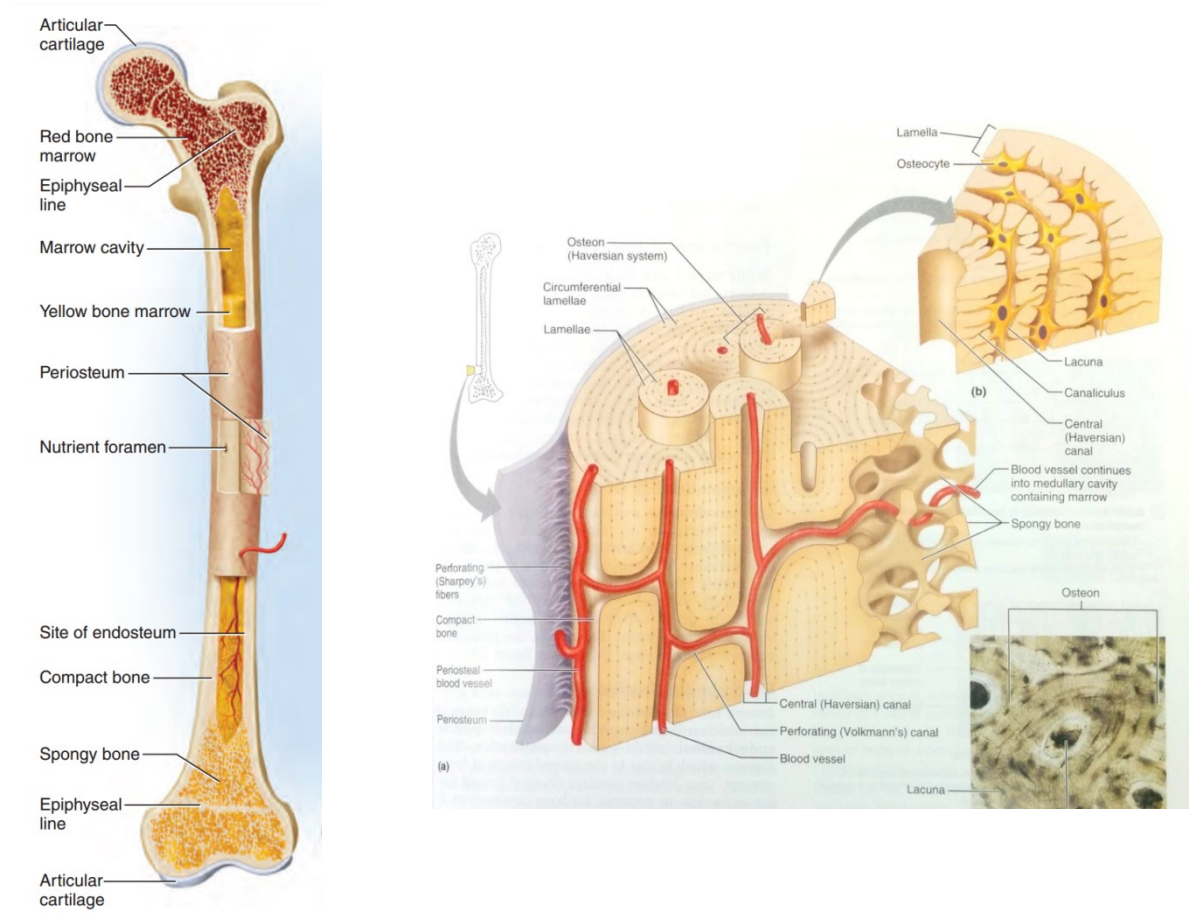

Figure 1: (A) ***Anatomy of long bone*** (Diagram from Kenneth S.Saladin. Anatomy and Physiology. 7th edition. New York: McGraw-Hill Education; 2015. Figure 7.1. Anatomy of a long bone) (B) ***Structure of osteon*** (Diagram adapted from Elaine N. Marieb. Human anatomy and physiology. 6th edition. San Francisco, CA: Pearson Education; 2004. Figure 6.6 a), Microscopic anatomy of compact bone)

1.3. Biology of bone

Bone is a dynamic and active tissue in the body that continually undergoes change in architecture throughout the life. The formation of bones, known as ossification takes place in the embryo, then bones continues to grow in thickness and length during infancy and early adulthood. In addition to their growth, bones are remodelled throughout the life to repair micro-fractures and maintain its integrity (1). Bone remodeling couples two processes; namely: the bone deposition and the bone resorption, both mediated by the synchronized function of different cellular participants in a sequential manner (4).

There are four main types of cells comprising bone that mediate the bone remodeling, namely: osteoblasts, osteoclasts, bone lining cells and osteocytes. Besides these cells, there are immune cells such as B-cells, T-cells, megakaryocytes and macrophages, which interact with bone cells and mediate the remodeling process. (5).

(I) Cells involved in bone remodeling

1. *Osteoclasts:* These are multinucleated cells that are differentiated from myeloid cells which play a role in removing mineralized bone matrix. The survival, expansion and differentiation of osteoclast precursor cells are primarily regulated by cytokines, CSF-1 (colony stimulating factor -1) and RANKL (receptor activator of NF- κB ligand). Osteoprotegerin (OPG), a soluble decoy receptor of RANKL functions as a negative regulator of osteoclast formation (6). Osteoclasts have a few distinct characteristics that define them; these include the expression of tartarate-resistant acid phosphatase and calcitonin receptor. Acid phosophatase is an enzyme that digests the collagen in bone matrix. Calcitonin receptor present on the surface of osteoclasts aids in the binding of calcitonin, a hormone that is secreted by the thyroid gland in response to a high level of calcium in bloodstream. (7).

2. *Osteoblasts:* These are specialized bone forming cells that play a role in bone modeling by expressing osteoclastogenic factors and producing bone matrix. There are two populations of osteoblast, the immature osteoblast lineage cells and the mature matrix-producing osteoblasts (8). The mature osteoblasts synthesize the organic matter of bone matrix, osteoid. A characteristic feature of osteoblast is the presence of parathyroid hormone

receptor on the cell surface which enables the binding of parathyroid hormone (PTH) that is released by parathyroid gland in response to low levels of blood calcium (7).

3. *Osteocytes:* A subpopulation of osteoblasts terminally differentiate and get engulfed in the unmineralized bone matrix (osteoid). After mineralization of bone, these entombed cells are called as osteocytes and are present inside fluid-filled cavities called lacunae. Osteocytes have dendrite-like processes called canaliculi, which extend throughout bone and helps in interacting with other osteocytes and osteoblasts, thereby forming a network throughout the bone. It is the osteocytes that surround the bone's blood supply, Haversian canal, and form an osteon (1). Osteocytes play multiple roles in bone. Some osteocytes resorb bone matrix, while the others help in formation of bone matrix, so they contribute in homeostatic maintenance of bone. More importantly, osteocytes play a key role as sensors of mechanical stress in bone. In presence of a mechanical load, the fluid in lacunae flow and stimulate the cilia on the osteocytes. This induces the cells to secrete signals for remodeling in order to adjust the bone shape to adapt to the stress (1, 9).

4. *Bone lining cells:* These cells are quiescent flat shaped osteoblasts that line the bone surface where no remodeling of bone takes place. The actual function of these cells remains elusive (5).

5. *Immune cells:* In addition to the bone cells, immune cells have also been reported to play a role in bone biology. B-cells, the central component of adaptive immune system, produces OPG (10) and thereby restrict osteoclastogenesis. Megakaryocytes, the platelet producing cells, enhances osteoblast formation, and also express RANKL and OPG, thereby playing a role in regulating both bone formation and resorption (11).

(II) Bone Remodeling

Bone remodeling takes place in the presence of a cluster of osteoblasts and osteoclasts arranged in a structure known as basic multicellular units (BMU) which is encased by bone lining cells. BMU provides an ideal microenvironment in which bone formation and resorption are coupled in order to ensure the maintenance of bone mass (12). The modeling of bone takes place in a sequential

process that involves five phases, namely: activation, resorption, reversal, formation and termination.

1. *Activation phase:* This is the initial phase of bone remodeling which begins in response to an initiating signal. The initiating signal can be of two types: (i) mechanical strain on bone or (ii) a hormone signal. In a resting state, osteocytes secrete transforming growth factor β (TGFβ) which inhibit osteoclastogenesis. When damage occurs in bone, it triggers the apoptosis of osteocytes which thereby reduces TGFβ and promote osteoclastogenesis for remodeling (13, 14). On the other hand, in response to reduced serum levels of calcium, parathyroid glands produce a hormone called parathyroid hormone (PTH). This hormone binds to PTH receptors present on the surface of osteoblasts which leads to the secretion of molecules that mediate bone resorption (15).

2. *Resorption phase:* In response to the PTH signal, osteoblasts secrete a chemokine monocyte chemoattractant protein 1 (MCP-1) which mediates the recruitment of osteoclast precursor (16). At the same time, OPG expression is reduced, RANKL, CSF-1 levels are increased in osteoblasts in response to PTH. These modulations lead to promotion of osteoclastogenesis and thereby bone resorption (17). In addition to these responses, signal, matrix metalloproteases (MMPs) are also secreted by the osteoblast in response to mechanical strain and PTH signal (18). MMPs degrade the osteoid and expose RGD (argenyl-glycyl-aspartic acid motif) adhesion sites which facilitates the binding of osteoclasts creating a microenvironment referred to as ‘sealed zone.' Hydrogen ions are pumped in this space leading to the dissolution of mineralized bone and forming a Howship’s resorption lacunae (6).

3. *Reversal phase:* At the end of resorption phase, the Howship’s resorption lacunae still remains covered with remnants of degraded matrix, which gets removed by mononuclear cells of unknown origin called reversal cells. This step leaves a space in the bone for subsequent bone formation by osteoblasts. Yet another role of these reversal cells is to facilitate the transition from bone resorption to bone formation in the BMU (4).

4. *Formation phase:* This phase is initiated by the signals from osteoclasts at the end of the reversal phase. Two important signals that are thought to be involved in initiating the transition from bone resorption to formation are sphingosine 1-phosphate and ephrin-B2 (EphB2) expressed by osteoclasts. Sphingosine 1-phosphate induce osteoblast maturation and EphB2 binds to the EphB4 receptor on osteoblast, enhancing osteogenic differentiation (19, 20) and activate bone formation.

5. *Termination phase:* Once an equilibrium is attained between bone resorption and formation, the remodeling process is terminated by signals that remain elusive (4).

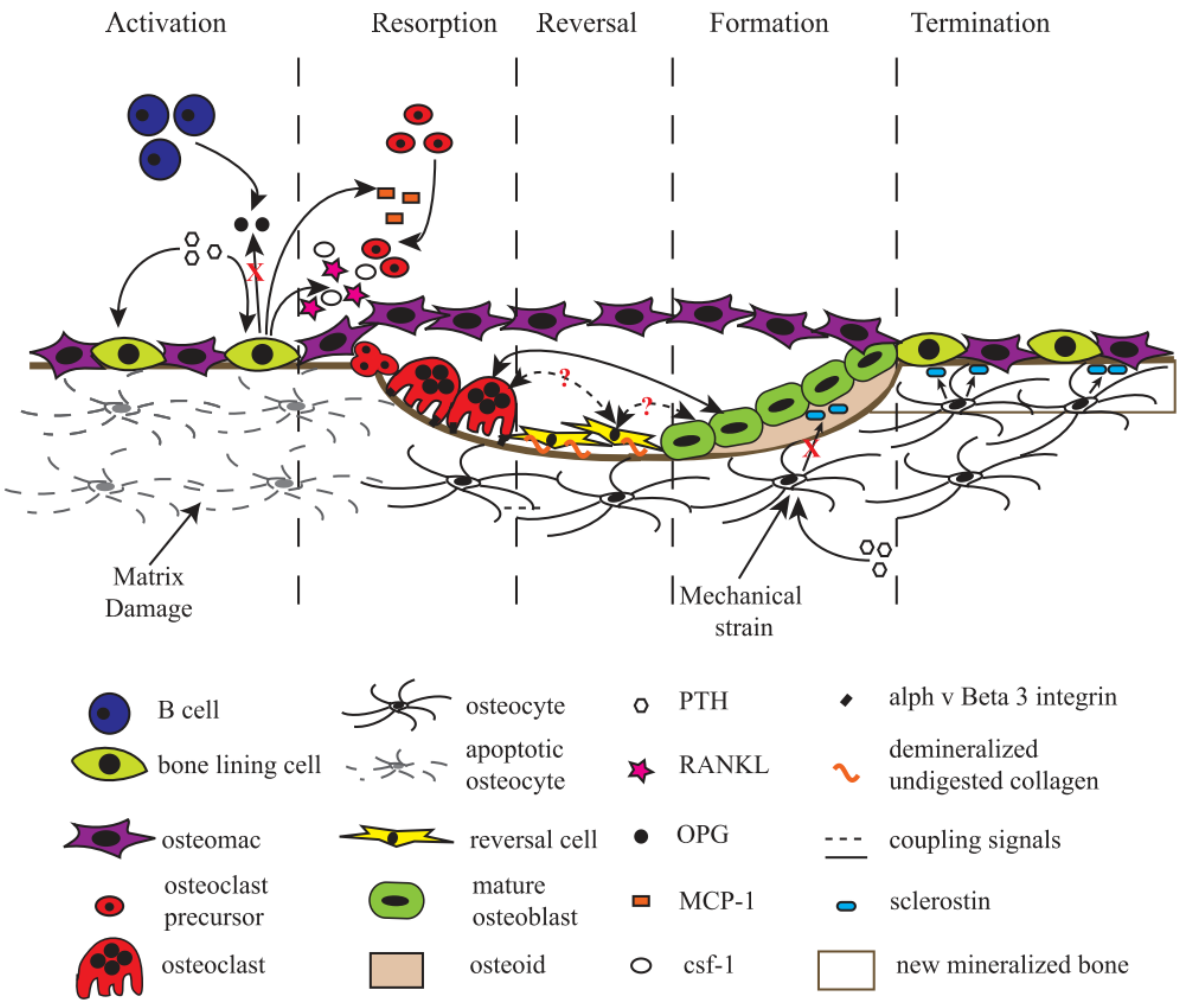

Figure 2: ***Process of bone remodeling***. At the resting phase, B-cells in the marrow produce OPG and osteocytes secrete TGFβ, which suppress osteoclastogenesis. In the *activation phase*, (i) endocrine remodeling signal or (ii) a mechanical strain reduces TGFβ to promote osteoclastogenesis. During *resorption phase*, osteoblast expression of OPG is reduced whereas RANKL and CSF-1 expression are increased promoting maturation of osteoclasts. Mature osteoclasts bind to the RGD sites on bone creating a sealed zone where osteoid is degraded. In the *Reversal phase,* reversal cells removes the degraded matrix and mediates the transition from resorption to bone formation. The *formation* is initiated by the signal that arises from degraded matrix and reversal cells. *Termination* halts the remodeling process by signals that are unclear.
Diagram adapted from Raggat LJ, Partridge NC, Cellular and molecular mechanisms of bone remodeling. J Biol Chem. 2010;285(33):25103-8. Figure 1, Schematic representation of a BMU and the associated bone remodeling process; p. 25105

1.2. Osteosarcoma

Osteosarcoma or osteogenic sarcoma (OS) is the most common primary bone malignancy with a high incidence rate in children and adolescents. Every year approximately 1300 children are diagnosed with cancer in Canada, and OS is the sixth most commonly diagnosed cancer among them (21). According to recent statistics, from 1992 to 2006 the number of OS incidences in children less than 14 years of age has been increasing gradually in Canada (22). OS predominantly occurs in the second decade of life with a median peak age of 16 years (23). However, it may also rarely occur in children less than 6 years and adults older than 60 years (24). The occurrence of OS is more common in the male population compared to the female population (25). Although the overall survival rate of OS patients has increased over the years, it still remains one of the childhood cancer with lowest overall survival rate (21, 22). Patients diagnosed with non-metastatic osteosarcoma have a better outcome, with an expected 5-year disease free survival (DFS) rate of 70% compared to an expected 5-year disease free survival rate of 20–30% in patients with metastases (26).

1.2.1. Etiology

(I) Genomic instability

Unlike other sarcomas that are characterized by specific genetic alterations, complex genomic alterations are involved in initiation of OS. Such complex alterations of genome is known as genomic instability. OS is commonly characterized by a type of genomic instability called chromosomal instability (CIN). CIN is defined as the high rate of change in the chromosome structure (Structural CIN) and number (Numerical CIN) in the cancer cells compared to normal cells (27). Mutation of mitotic checkpoint genes, such as tumor protein 53 (TP53), retinoblastoma (RB), mouse double minute 2 homolog (MDM2) and cyclin dependent kinase 4 (CDK4), is a major reason for CIN. p53 and Rb proteins are tumor suppressors, whereas Mdm2 and Cdk4 proteins act as negative regulators of p53 and Rb respectively. Studies have reported genetic alterations of p53, pRb, MDM2 and CDK4 in OS patients (28-32). Besides these cell cycle related genes, it has been reported that RECQL4 gene which encodes for DNA helicase is associated with structural CIN in OS patients (33). A comprehensive review on the genetic alterations reported for OS is given by Martin *et. al.* (34).

(II) Inherited syndrome

Although many reported OS cases are due to sporadic genetic alterations, a familial link has also been associated with the occurrence of OS. Patients with inherited genetic syndromes such as retinoblastoma, Li-Fraumeni syndrome and Rothmund Thomas syndrome have a higher proclivity to develop OS (35).

(III) Other rare factors

Rarely, other factors have also been implicated to promote OS. Radiation has been cited to induce OS. However, OS occurs in this case, approximately 20 years after the initial exposure (36), therefore making it questionable. A viral etiology is also thought to promote OS. SV40 (Simian Virus 40) gene has been detected in OS patients by PCR (37).

1.2.2. Anatomical sites of Osteosarcoma

The anatomical sites for OS are widely distributed in the skeletal system. The majority of primary OS occur in long bones of the body, the most common sites being femur (42%), tibia (19%) and humerus (10%). Occasionally, primary OS may occur in the jaw (8%) or pelvis (8%) and very rarely in ribs (1.25%) (25).

1.2.3. OS - tumor formation and appearance

As mentioned earlier, OS predominantly occurs in the long bones during adulthood. OS usually begins at the intramedullary (inside the medullary cavity) region of bone and slowly grows radially as a ball-like mass. The tumor growth may be limited to the medullary region, however in most cases extends to the cortex, resulting in compression of the surrounding muscles and form a pseudocapsular layer referred to as ‘reactive zone’ (38, 39).

1.2.4. Types of OS

OS is simply defined as a mesenchymal tumor in the connective tissue that produces immature bone matrix (also referred to as tumor bone or tumor osteoid). OS is subdivided into many types. Based on the type of occurrence, it is classified as primary (initial tumor) or secondary (lesion arising from an existing tumor). Based on location, OS is broadly classified as intramedullary and surface OS. Although OS typically arises in the medullary cavity of the long bone, occasionally it also arises on the surface of the bone. As illustrated in Figure 3, intramedullary OS is further classified into conventional, telangiectatic, small cell, or low grade. Surface OS is divided into Parosteal, periosteal and High-grade surface OS.

(I) Intramedullary OS

1. *Conventional OS:* This is the most common type of OS which typically occurs in the long bones and is aggressive in nature. The tumor cells produce osteoid mass which causes an increased thickness in some areas of bone. This is called as sclerotic lesion and due to its thickness it is difficult for the x-rays to penetrate the mass. Such a radiodense mass is a characteristic feature of conventional OS. Histologically, the tumor cells appear to be spindle-shaped with a pleiomorphic nucleus. Conventional OS is further sub-divided into chondroblastic, osteoblastic and fibroblastic depending on the appearance of the matrix. If the osteoid is entrapped with neoplastic osteoblasts, it is osteoblastic OS. However, if chondrocytes are present in the matrix, it is chondroblastic OS. In addition to these, atypical spindle cells admixed with tumor cells are known as fibroblastic OS _ENREF_38(35, 40, 41).

2. *Telangiectatic OS:* This type of OS accounts for 3% of OS and is quite different in nature compared to conventional OS. Unlike conventional OS which is characterized by a sclerotic mass, telangiectatic OS is characterized by cystic cavities. Hence, the radiographic appearance is characterized by a radiolucent (transparent to X-rays) bone destruction accompanied with an asymmetric expansion of bone. The cyst cavities are generally composed of multiple blood-filled sinusoids. Due to the extensive destruction of bone mass, patients often present with bone fractures at the time of diagnosis (42, 43).

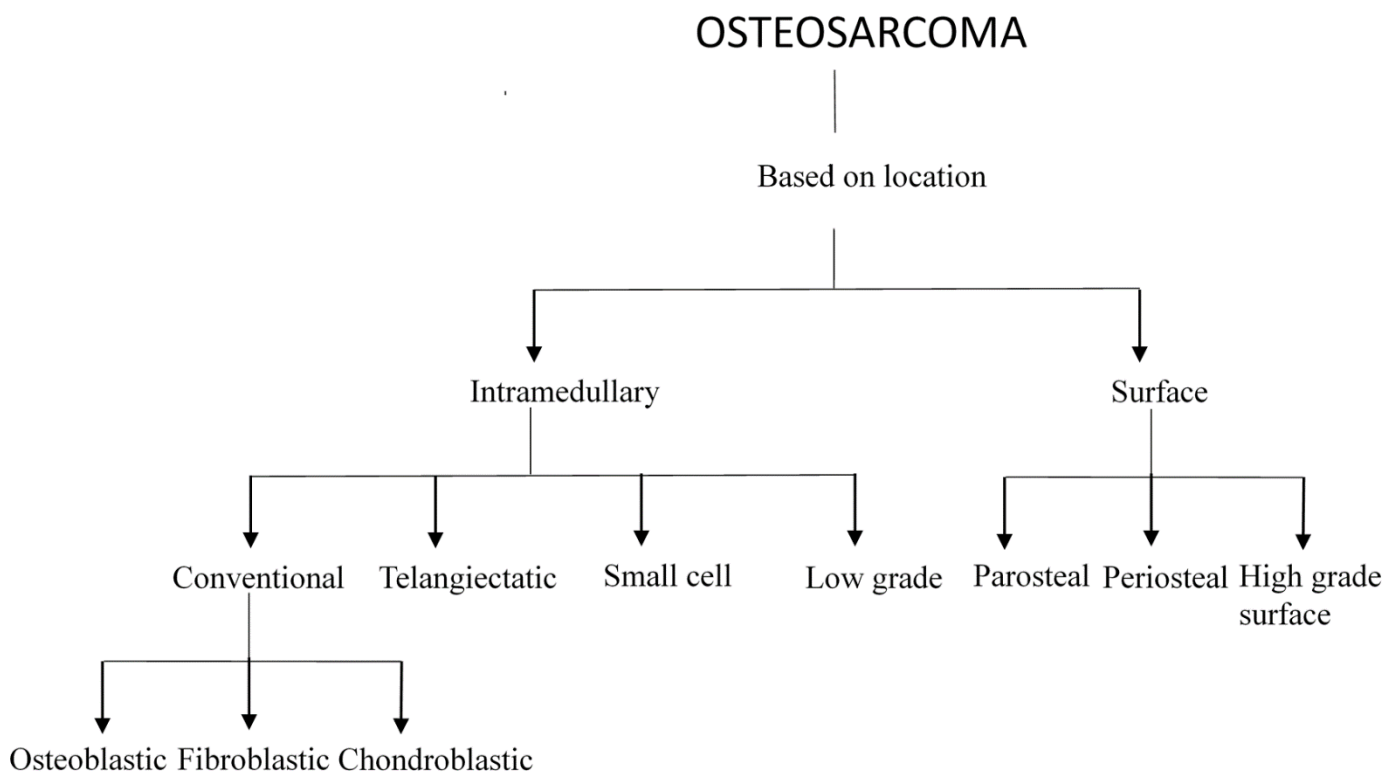

Figure 3: ***Classification of Osteosarcoma***

3. *Small cell OS:* This type of OS is very rare and constitutes only 1-2% of all OS. The radiological appearance of small cell OS is very uncharacteristic of a typical OS, as small cell OS has minimal mineralized matrix. Histologically, Small Cell OS closely resembles Ewing sarcoma, constituted of small, round cells with insignificant pleomorphic nuclei. Also, similar to Ewing sarcoma, small cell OS sometimes present with a positive membrane staining for CD99 and a reciprocal translocation between chromosome 11 and 22 similar to Ewing sarcoma. However, regardless of these similarities with Ewing sarcoma, small cell OS differs significantly in its response to radiation. While Ewing sarcoma responds well to radiation, small cell OS is insensitive to this treatment approach (40, 44).

4. *Low-grade OS:* It is the only type of OS in the intramedullary location that is low grade histologically and is slow in terms of progression. Similar to conventional OS, it is typically located in the tibia or femur (35).

(II) Surface OS

Bones are covered with an outer and inner membrane which are called periosteum and endosteum respectively. Surface OS tumors are basically located on the surface of the bone and therefore, the lesion would be associated with the periosteum.

1. *Parosteal OS:* This is a slow growing lesion found on the surface of the bone, commonly on the posterior distal femur. Clinically, patients present with an indolent mass of tumor in the knee region with no symptoms of pain. Radiographically, the tumor appears as a sclerotic, well-defined lesion on the bone that presents with a "stuck on the bone" appearance (35). The tumor tends to be more radio-dense as it approaches the bone surface and less dense peripherally. Mostly these tumors are associated with the fibrous outer layer of periosteum (45).

2. *Periosteal OS:* This type of OS is less common compared to parosteal OS. The major difference of periosteal OS from parosteal is the location of the tumor. Periosteal OS has a lesion that is associated with the inner cambium layer of periosteum, unlike parosteal OS in which lesion is associated with the fibrous outer layer as mentioned before (46).

1.2.5. Symptoms

The most common presenting symptom of OS is pain. A retrospective study that aimed at establishing initial symptoms for OS reported pain to be the first detectable symptom in OS patients. 85% of patients reported pain at the point of initial examination (47). The patients typically present with dull pain for several months which becomes severe with the course of time. The severity in pain is related to the penetration of cortical bone by the tumor mass. While night pain is common, patients may also have frequent occurrences of minor injury, sprain etc. while participating in activity (39). The second clinical symptom in OS patients is swelling, about 40% of patients presented with a palpable mass (47). Other clinical presentations are localized tenderness and restrictive movement of the adjacent joint. Besides these medical symptoms, there are a few biochemical changes that are associated with OS. Serum lactate dehydrogenase (LDH) level is a biochemical marker for OS. Patients with metastatic condition at the time of diagnosis have elevated serum LDH levels compared to patients with localized tumor (48). Increased levels of serum alkaline phosphatase (AP) is also reported to be associated with OS (49, 50).

1.2.6. Diagnosis for OS

Patients presenting with clinical symptoms such as pain, fracture or swelling of bones lead the physicians to further examine for presence of tumor in bone. Imaging is the primary diagnostic approach for OS. Different imaging techniques are used to identify the presence of tumor and to obtain information critical to evaluate the extent of tumor spread (51). The process of judging the speed and extent of growth of a tumor is called staging. Currently used imaging techniques for OS diagnosis are:

1) Radiography
2) Computed Tomography (CT)
3) Magnetic Resonance Imaging (MRI)
4) Nuclear Medicine Scintigraphy

The first step in diagnosis, is to carry out a radiography (X-ray) on the area of bone that is suspected for the presence of tumor. If radiography evaluation is negative but the patient continues to present with symptoms, an MRI is carried out. In the event the patient is not suitable for MRI, a CT or

Tc99 mMDP (methylene di-phosphonate) bone scan is carried out. If the initial radiographic evaluation is positive, MRI is carried out to determine the extent of tumor progression. Preceding the careful examination of imaging results, a biopsy is done for histologic diagnosis.

(I) Radiography

Radiography is based on the degree of attenuation of X-rays by tissue. In this modality of imaging, patients are exposed to X-rays, which gets absorbed by the tissue depending on the density of tissues. The rays that pass through the tissue are captured by a detector, and a superimposed 2D image is acquired. Radiographic evaluation of OS is based on Lodwick's classification system which depends on four main characteristics, namely: i) destruction of bone ii) proliferation of bone iii) tumor matrix and iv) shape and size of the tumor (52).

Advantages:

i) Provides excellent resolution

ii) Helps in assessment of lesion characteristics

iii) Helps distinguishing aggressive and non-aggressive tumor

iv) Less cost associated

Limitations:

i) Medullary lesions may not be visible. Long bones are comprised of cortical bone that envelops cancellous bone and central medullary cavity. Radiography is useful in visualizing the lesions in cortical or cancellous bone. However, it is insufficient to detect medullary lesions as they are interior.

ii) The extent of tumor involvement in surrounding tissues cannot be assessed as the density of tumor, and the surrounding tissue is similar, and hence attenuate X-rays to the same degree (53).

(II) Computed Tomography

CT works on the same principle as radiography by using X-rays. However, it utilizes sophisticated computer algorithms to generate images with more detail and clarity. Acquisition of image from CT is carried out by passing X-rays from various directions onto each slice of tissue, which is projected onto detectors. The detectors send these signals to a computer, which processes the signal using algorithms and produce a clear image of the scanned tissue.

Advantages:

i) Possible to visualize medullary lesions (54)

ii) Allows determination of the extent of soft tissue involvement with the bone tumor (54)

iii) Quick speed of acquisition reduces motion artifacts

Limitations:

i) Higher radiation dose than conventional radiography; use should be limited in young children and pregnant women

ii) Extent of bone marrow involvement cannot be acquired with clarity

iii) Distant metastases may not be accurately determined. A retrospective study which evaluated the efficiency of CT in detecting metastases in lungs showed CT to underestimate the number of metastases (55).

iv) Inability to provide histologic information (53)

(III) Magnetic Resonance Imaging

Traditionally, MRI is the imaging technique that has been used for staging of bone tumors. MRI uses magnetic properties of protons and radiofrequency pulses in a high magnetic field to acquire images of tissue.

Advantages:

i) Helps in assessment of the extent of bone marrow involvement

ii) Provides details on discontinuous metastases in the same bone (skip metastases)

Lack of ionizing radiations

Limitations:

i) Artifacts from metallic objects. Patients with OS have might have metallic hardware after surgery which might cause artifacts on MRI (53).

ii) Limited detection of calcification

(IV) Nuclear Medicine Scintigraphy

Bone scintigraphy is a very useful technique for detecting distant metastases. This technique uses isotopes for acquiring images. Technetium 99 Methylene Diphosphonate (MDP) is the commonly used isotope for bone scintigraphy. Yet another known radiotracer used in the diagnosis of bone

tumor is Fluorine 18 – FDG (Fludeoxyglucose), which is a radiolabeled glucose analog. This tracer inherently gets incorporated in cells that are metabolically active and hence the tracer has a predilection for tumor cells. A PET/CT scan is used to image the anatomic localization of the tracer in body. FDG/PET is shown to be useful in detecting OS at its primary tumor and distant metastases (56).

1.2.7. Staging of OS

OS is staged based on the Enneking staging system, in which the malignant tumor is assessed based on 3 factors

1) Surgical grade – G1, G2
2) Local extent – T1, T2
3) Metastasis – M0, M1 (Absence of metastasis – M0, presence of metastasis – M1)

According to the Enneking staging system, there are 3 stages of tumor with I and II being non-metastatic and III being a tumor with metastases at distant sites. Tumors are further classified into two grades, low grade (G1) or high grade (G2). Low-grade tumors have less than 25% risk of spreading whereas high-grade tumors have a high incidence of spreading. Based on the location, tumors are further classified as intra-compartmental (T1) and extra-compartmental (T2). Tumor that is grown within the cortex of bone is intra-compartmental, whereas if tumor has grown outside the cortex, it is extra-compartmental. Several histologic and radiologic features are taken into account in order to grade a tumor. Histologic features include mitotic rates, nuclear to cytoplasmic ratio and pleomorphism, whereas radiographic features include assessing for the anatomical confines of the tumor using imaging techniques (57).

Stage	Grade	Site	Metastasis
IA	Low (G1)	Intracompartmental (T1)	No metastasis (M0)
IB	Low (G1)	Extracompartmental (T2)	No metastasis (M0)
IIA	High (G2)	Intracompartmental (T1)	No metastasis (M0)
IIB	High (G2)	Extracompartmental (T2)	No metastasis (M0)
III	Any (G)	Any (T)	Regional or distant metastasis (M1)

Table 1 – Enneking's staging system for malignant musculoskeletal tumors (Table from Jawad MU, Scully SP. In brief: Classifications in brief: enneking classification: benign and malignant tumors of the musculoskeletal system. Clin Orthop Relat Res. 2010;468(7):2000-2. Table 2, Enneking staging for malignant musculoskeletal tumors based on surgical grade, local extent and presence or absence of metastasis; p 2001)

1.2.8. Current clinical treatment for OS

The clinical treatment plan for OS involves a combination of various approaches such as surgery, chemotherapy, and radiotherapy. Chemotherapy and radiotherapy are combined with surgery in a pre-operative or post-operative manner. The treatment plan depends on the type of OS. For patients with high-grade OS, treatment includes preoperative (neo-adjuvant) chemotherapy, surgery and postoperative (adjuvant) chemotherapy. Surface tumors like parosteal OS are primarily treated with surgical resection, while chemotherapy is reserved for cases of high-grade transformations. On the other hand, periosteal OS is treated with pre-operative chemotherapy followed by surgery (58).

(I) Surgery

Surgery has been the cornerstone treatment approach for OS. Imaging techniques like CT and MRI are used for planning the surgical margins prior to the surgical procedure. The surgical margin should comprise the tumor, the reactive zone and a cuff of surrounding normal tissue. Two surgical procedures used for OS to excise tumor are:

1) Amputation – Surgical removal of the entire limb that is affected by tumor.
2) Limb salvage – Surgical removal of the affected part of limb to preserve the functioning limb without increasing the possibility of tumor recurrence.

Several studies have reported no significant difference between the survival rate of patients with amputation vs. limb-salvage surgery (59-61). A study by Grimer *et.al.* observed an increased occurrence of local recurrence in patients undergoing limb salvage surgery compared to patients undergoing amputation, yet there was no difference in survival rate between the groups (62). Limb salvage surgery is the preferred option of surgical procedure for OS if the tumor margins are defined. In cases where the tumor margin is not clear, amputation is preferred to prevent local recurrence.

(II) Chemotherapy

Treatment for OS has evolved over the last 40 years. Until 1970, OS was considered to be chemo-resistant as the response to various chemotherapeutic drugs like mitomycin C (63), cyclophosphamide (64), vincristine (65, 66), 5-flurouracil (67) was poor and inconsistent. Therefore, amputation was the primary treatment option for OS. However, in the mid-1970s,

doxorubicin (68) and methotrexate (69) proved to be effective and since then a combination of chemotherapeutic agents have been used for OS treatment (70). Currently, the most commonly used chemotherapeutic drugs for OS are Doxorubicin, Methotrexate, Cisplatin and Ifosfamide. Chemotherapeutics drugs are administered in a systemic manner through intravenous or rarely intra-arterial route. The standard treatment regimen used for non-metastatic OS is a combination of pre-operative and post-operative chemotherapy. The chemotherapy is administered prior to surgery (neo-adjuvant) to induce necrosis in the primary tumor, which helps in surgical resection and acts as an early treatment to limit micro-metastases. Adjuvant chemotherapy is effective in improving the disease-free survival rate for patients with non-metastatic condition (71).

Various studies have reported the response of patients to different strategies of administering chemotherapy. Patients have improved response when combinations of chemotherapeutic agents are administered (72). However, increasing the dosage of drugs does not improve the response of patients (73). While adjuvant chemotherapy using multiple drugs is effective for patients with skip metastases, it is ineffective for the survival of patients with multifocal synchronous OS (OS with multiple metastases but no lung metastases) (74) (75). Despite the combined treatment strategies currently used in the treatment of OS, recurrence and metastases still arise in about 30-40% of patients, which is the major reason for death. Time of relapse depends on the serum AP levels, type of chemotherapy administered and histologic response to preoperative chemotherapy (76).

(III) Radiotherapy

Radiotherapy is not a widely recommended treatment approach for primary OS unless lesions are present in inaccessible regions. However, radiation treatment is sometimes administered prior to biopsy in order to reduce the viability of cancer cells that may disseminate into the bloodstream due to the biopsy procedure. One of the major advances in the field of radiotherapy for OS is extracorporeal irradiation, in which bone is taken out of the body, irradiated and re-implanted. Major advantages of this treatment are, a lack of graft rejection or risk of viral transmission (38, 77).

1.2.9. Prognosis

The advent of chemotherapy in the treatment of OS had significantly improved the survival of patients since the mid-twentieth century. In the pre-chemotherapy era, long-term survival rates were lower than 20%, which has been significantly improved to about 60-65% with the incorporation of chemotherapy in treatment regimens (63). Although the survival rate of patients has tremendously improved over years, it has reached a plateau in the last two decades. Therefore, it is pivotal to identify reliable prognostic markers and therapeutic targets to improve the disease free survival of OS patients.

Our understanding of the pathobiology of OS has accrued over years, which in turn has facilitated the finding of several candidate genes/proteins with potential prognostic and therapeutic value. The next few sections of this chapter will discuss the pathobiology of OS and how the knowledge of the biology of this disease has been translated to find prospective prognostic markers and therapeutic targets.

1.2.10. Biology of OS

In OS, the regulated process of bone remodeling orchestrated by osteoblasts and osteoclasts is lost, thereby leading to the formation of immature bone mass by the tumor cells. Extensive research on understanding the tumorigenesis of OS has led to the identification of various players involved in each stage of disease progression and the underlying mechanism. This section will discuss the current understanding of biological mechanisms involved in each hallmark of OS progression.

(I) Tumor initiation:

Several molecular changes take place in normal cells which transforms them into a neoplastic state. The molecular events that are involved in initiating OS tumor are (i) over-activation of growth signalling pathways, (ii) genetic alterations of tumor suppressor genes, and (iii) overexpression of proto-oncogenes. There are many growth signaling pathways in cells that promote cell growth and proliferation. In normal cells, these signaling pathways are tightly regulated in order to maintain controlled cell growth and proliferation. Growth signaling pathways like the transforming growth factor β (TGFβ) and insulin growth factor (IGF) are upregulated in OS. TGFβ-1 is highly expressed in high grade OS (78). Similarly, IGF signaling is also upregulated in OS cells. A study by Burrow

et.al, showed increased expression of IGF ligand and IGF receptor in OS patients, however, there was no correlation with metastasis (79, 80). *In vitro* studies have shown that OS cells express IGF receptor on their surface, which when blocked by monoclonal antibodies reduce their growth *in vitro* (80). In addition to deregulation of the aforementioned growth signaling pathways which promotes cell growth and proliferation, genes that mediate cell apoptosis are downregulated in OS cells. P53 and RB (Retinoblastoma) genes are key tumor suppressor genes that plays important roles in regulating cell cycle and apoptosis in normal cells. Rb is a cell cycle regulator that controls cell cycle progression from G1 to S phase by binding to a transcription factor called E2F. E2F remains inactive by the binding of Rb until CDK4/CyclinD (Cyclin dependent kinase 4 / CyclinD) complex phosphorylates Rb. Loss of heterozygosity (deletion of an allele of a gene) of RB gene is reported in OS patients (81). Besides loss of RB gene, an increased expression of CDK4, a regulator of Rb, is also reported in OS patients. A study which analyzed the expression of CDK4 in 20 OS patients found 65% of patients to highly express CDK4 (29). Another key player in cell cycle regulation is p53, a protein that mediates cell cycle arrest by cell apoptosis. Point mutations and missense mutations of P53 have been reported in OS patients (28, 30, 31). However, the p53 mutation status did not differentiate patients with localized OS and patients presenting with metastatic condition. This indicates that p53 mutation is not a late event as it is established prior to metastases formation (31). Besides the above discussed regulators of cell proliferation and apoptosis, another point of regulation is mediated by transcription factors. c-myc, c-fos and c-jun are transcription factors which mediate cell proliferation and growth in response to growth signaling. c-fos and c-myc are reported to be highly expressed in OS patients (82, 83). Cumulatively, the upregulation of growth signaling and suppression of cell apoptosis lead to the unregulated proliferation of cells and form a tumor. β-catenin, the regulatory molecule of Wnt signaling pathway is also known to be involved in initiating OS. The current understanding about the role of β-catenin in OS will be discussed in detail in later sections of this chapter.

(II) Neo-vascularization:

A tumor, once formed, requires a supply of nutrients and oxygen in order to sustain and grow. This demand is met by the formation of new blood vessels within the tumor, a process referred to as neo-vascularization. The cells inside a tumor mass are deprived of proper oxygen supply. Such hypoxic conditions inside OS tumor trigger the expression of a transcription factor Hypoxia

induced factor-1 (HIF-1) and upregulates the expression of Vascular endothelial growth factor (VEGF) (84). VEGF is a pro-angiogenic factor that plays a vital role in the development of vasculature. A study by El Naggar *et.al.,* showed increased expression of HIF-1 in OS cell lines compared to normal osteoblasts and confirmed the observation in OS patients with immuno-histochemical staining for HIF-1 (85). Gene amplification of VEGF-A is reported in OS patients (86) and is found to be correlated with poor prognosis of patients (87, 88). The expression of HIF-1 and VEGF-A increases in OS tumor, thereby promoting angiogenesis to aid in tumor survival.

(III) Invasion*:*

Invasiveness is a crucial characteristic that tumor cells acquire in order to spread from the primary tumor site. In order to metastasize to a different organ from the tumor site, cells must enter the bloodstream by breaking the basement membrane at the tumor site and extracellular matrix. The process of tumor cells invading the basement membrane, extracellular matrix and entering the blood vessel is called invasion. Tumor cells express increased level of enzymes like matrix metalloproteases (MMP) and serine proteases. MMP function in degrading the extracellular matrix, which enables tumor cells to invade the membrane and enter the bloodstream. OS cells express upregulated levels of MMPs, especially MMP2 and MMP9 (89-92) and are known to be of prognostic importance in OS. Urokinase plasminogen activator (uPA) is a serine protease that converts the zymogen plasminogen into active plasmin, a protease that degrades the extracellular matrix (93). OS cells express high levels of uPA (urokinase plasminogen activator), which favors tumor spread (94, 95).

(IV) Anoikis resistance:

Tumor cells that enter the bloodstream lack cell-cell and cell-matrix interaction. As a barrier to metastasis, cells that lose contact with neighboring cells or extracellular matrix are targeted to apoptosis. This process of cell death of the anchorage independent cells is called anoikis (96). There are several mechanisms by which anoikis is mediated in anchorage independent cells. One of the most important mechanism is through integrin signaling. The biological functions of cell-extracellular matrix interactions contacts are largely mediated by integrin type of receptors. There are 18α and 8β integrins that have been identified in humans. These integrins associate in a non-covalent manner with each other to form 24 different αβ heterodimer receptors. Integrins with β1

are those that act as receptors for extracellular matrix components. Unlike most receptors, integrins are non-kinase receptors. Therefore, they require a kinase downstream to mediate the signaling. Focal adhesion kinase (FAK) is one such kinases that help in mediating the signal after the binding of an extracellular matrix ligand to integrin. Recruitment of FAK by the integrins lead to the recruitment of Src. Such integrin mediated FAK/Src signaling mediates several pathways downstream including the phosphoinositol 3 kinase (PI3K) pathway and mitogen activated protein kinase (MAPK) pathway etc., which leads to increased expression of anti-apoptotic homologs and decreased expression of pro-apoptotic homologs (97). This prevents the anoikis of anchorage independent tumor cells and favors their sustenance in bloodstream. An in-vitro study showed expression of α4β1 integrin in SaOS cell line. Cells that were not adherent were seen to be targeted for anoikis, which was increased when the α4 integrin was blocked with a α4 integrin monoclonal antibody (98). This study suggests a role of integrin in mediating anoikis in OS cells.

(V) Extravasation:

Disseminated tumor cells (DTC) that survive in the bloodstream extravasate at a distant organ from the primary tumor, which in OS is predominantly the lungs. The invasion of OS cells into the lungs is dependent on the conducive environmental factors present in lungs. OS cells over-express a chemokine receptor CXCR4 (C-X-C chemokine receptor type 4) (99, 100) which assists the binding to CXCL12 (C-X-C-chemokine ligand 12) expressed by lungs and facilitates colonization of OS cells. Another protein which plays a key role in the metastasis of tumor cells in OS is Ezrin. Ezrin is a membrane-cytoskeleton linker protein that is inactive in the cytoplasm, which upon tyrosine or threonine phosphorylation becomes active and moves to membrane. Ezrin is reported to be upregulated in OS (101-104) and is correlated with poor prognosis in OS patients. Ezrin's linkage of cell membrane to the actin cytoskeleton aids the cell to interact with its microenvironment and thereby helps in mediating cell signaling by growth factors. A study from Khanna *et.al.,* examined role of ezrin in OS metastasis by knock down experiments. In this study, the murine osteosarcoma cell line K7M2 was stably transfected with full length anti-sense ezrin and mutant ezrin-T567A (which cannot be phosphorylated and hence cannot become active) and the transfected cells were injected into mouse for studying the metastatic potential. The knockdown of ezrin significantly diminished metastases formation in mouse without any changes in in-vitro proliferation of cells or primary tumor formation in-vivo. Imaging studies using inverted

fluorescent video microscopy, which examined the tumor cells metastasizing to lung, showed no changes between wild type ezrin and the knock down conditions at 3 hours, but the number of cells metastasizing to lung decreased fourfold at 6 hours and not detectable after 24 h in the knock down condition. It was also found that cells with knock down ezrin had decreased kinase activity of MAPK and AKT. However, with activation of MAPK pathway, 51% of the early metastatic potential that was lost in knock down condition was recovered. Thereby, this study demostrated the role of ezrin in sustaining the OS cells by mediating the MAPK pathway and aid in metastasis of OS cells to lungs (105).

(VI) Chemoresistance:

Despite the advances in chemotherapy treatment modules for OS, the disease-free survival for patients with metastatic condition remains poor. One major reason for poor survival is the resistance to chemotherapy acquired by OS patients with time. OS cells express increased levels of P-glycoprotein (106), a transmembrane ATP-dependent efflux pump which allows multidrug resistance. This leads to poor response of patients to the existing chemotherapeutic drugs.

(VII)Vicious cycle of OS:

An important biological phenomena in the progression of OS is the vicious cycle of activity of the bone cells, osteoblasts and osteoclasts. In normal bone, a balance between the bone formation by osteoblast and the bone resorption by osteoclasts are tightly regulated (section 1.1.3). This balance is lost in OS. OS cells are known to produce RANKL (107, 108), so they can directly activate osteoclasts without osteoblasts. Tumor cells produce factors like PTHrP, IL-1, IL-6, etc. which induce osteoblasts to express RANKL and aid in activation of osteoclast precursors. The activated osteoclasts degrade the bone matrix, which leads to the release of growth factors like TGFβ and IGF. These growth factors act on tumor cells and stimulate the release of PTHrP and interleukins that stimulates osteoclasts. This vicious cycle is key for the progression of OS (109) (Figure 4).

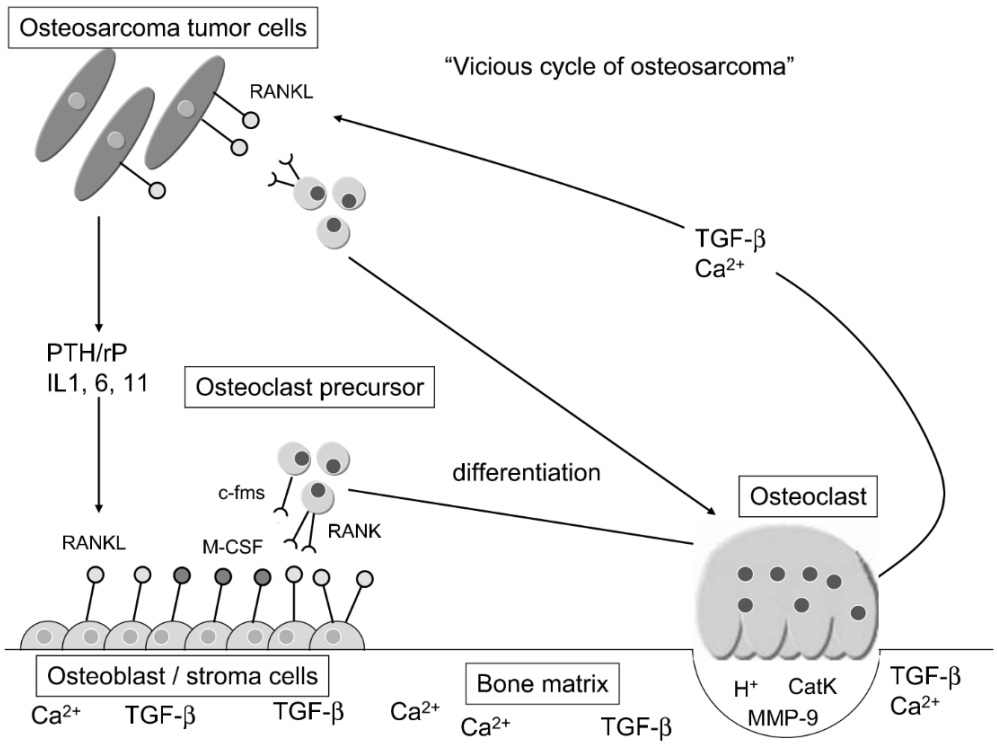

Figure 4: ***Vicious cycle of osteosarcoma***. Osteosarcoma cells produce RANKL that aids in the osteoclastic activity directly without osteoblasts. On the other hand, OS tumor cells also produce PTHrP and IL which causes increased expression of RANKL by osteoblasts and thereby promotes osteoclastic activity. The increased osteoclastic activity aid in degradation of bone matrix, releasing growth factors like TGFβ and IGF. These growth factors act on tumor cells and further stimulate the release of PTHrP and IL, and cause more osteoclastic activity. Diagram adapted from Akiyama T, Dass CR, Choong PF. Novel therapeutic strategy for osteosarcoma targeting osteoclast differentiation, bone-resorbing activity and apoptosis pathway. Mol Cancer Ther. 2008;7(11):3461-9. Figure 1,Vicious cycle of osteosarcoma; p 3463.

1.3. Developments in biomarker and targeted therapy for OS – Current scenario

Advancement in the understanding of OS pathobiology has shed light on the mechanism and key molecular players mediating OS progression. This has led to the identification of biomarkers and putative therapeutic targets. Currently, numerous prognostic markers have been identified for OS, which might be broadly classified into two groups, based on their predictive role: (i) markers with potential value in predicting the course of disease and (ii) markers with potential value in predicting response to a treatment module. Based on the literature, some of the known markers that might be helpful in predicting OS progression are survivin, P53, VEGF, ezrin, MMP2, MMP9 etc. On the other hand, marker like P-glycoprotein is predictive of response to chemotherapy. An elaborate list of currently known prognostic markers is provided in Table 2.

Translation of our current knowledge on the mechanisms of OS genesis and progression has also been pivotal in the development of targeted therapy for OS. Some of the major landmarks in targeted therapy for OS are (i) IGF-1R targeting drugs: inhibits the highly activated IGF signaling in OS; (ii) VEGF inhibitors: dampen angiogenesis and hence halt the blood supply required for tumor survival and growth; (iii) Zoledronic acid: attenuates the increased osteoclast activation in OS; (iv) ABC transporter (ATP-binding cassette transporter) modulators: combats the drug resistance offered by OS cells. Many of the drugs and inhibitors has been tested *in vitro* and *in vivo* for their effectiveness against OS and some of them have advanced to clinical trials (Table 3).

While recent research on markers for OS progression has identified several potential markers for disease progression, there are no reliable prognostic markers for OS that are currently used in clinic. Therefore, expanding our understanding about molecular players in OS pathobiology will aid in identifying more clinically relevant prognostic markers for OS. In light of this, the current study is focused on understanding the role of key regulators of Wnt signaling pathway, β-catenin and active β-catenin (ABC), in OS progression.

Identified biomarkers	Function	Prognostic significance	Reference
Proto-oncogenes			
c-MYC	Transcription factor – regulates expression of genes involved in cell growth and apoptosis	Over-expression in patients metastasis and relapse	(83)
c-FOS	Transcription factor – regulates expression of genes involved in cell proliferation, hypoxia, angiogenesis	Over-expression in patients metastasis and relapse	(82, 83)
Growth signaling			
TGFβ	Cell growth	High expression of TGFβ-1 in high-grade OS	(78)
IGF	Cell growth	Increased expression of IGFR and IGF – No change in expression with metastasis	(79)
Apoptosis			
P53	Promotes cell death	Alterations associated with OS. Not associated with metastasis.	(30, 31, 110)
Livin	Anti-apoptotic	Expression associated with overall survival	(111)
Survivin	Anti-apoptotic	Localization of survivin is predictive of survival	(112)
Cell cycle			
CDK4	Promotes G1-S phase progression in the cell cycle. Function depends on CyclinD and p16.	Increased expression associated with OS but not in metastasis	(29)
Rb	Negative regulator of cell cycle G1-S phase	Alterations associated with OS	(28)
INK4A (P16, P14)	P16 – inhibits CDK4 – arrest cell cycle progression P14 – sequesters p53 – promotes apoptosis	Deletion or absence associated with poor survival	
MDM2	Binds and degrade p53	Amplification associated with metastasis of OS	(28, 32)
Angiogenesis/Hypoxia			
VEGF	Promote formation of blood vessels	High expression associated with metastasis and recurrence	(84, 86)
HIF-1	Transcription factor – regulates expression of genes in survival for cells in hypoxia	Increased expression in OS	(85)
Cell adhesion			
Ezrin	Links cell membrane to the cytoskeleton. Helps in mediating signal and promote metastasis	Increased expression associated with OS metastasis	(101, 102, 105)
CD44		Increased expression associated with OS metastasis	(113)
Extra cellular matrix			
MMP	Degrade extracellular matrix	Expression of MMP2, MMP9 associated with poor survival	(90-92)
uPAR	Promote the degradation of extracellular matrix	Expression of uPAR associated with metastasis	(94, 106)
Drug resistance			
p-Glycoprotein	Cellular drug efflux	Doxorubicin resistance	(106)

Table 2: Currently identified biomarkers for OS and their prognostic significance

Drug	Company	Target	Mechanism of action	Stage of development
Monoclonal antibodies (mAB)				
Robatumumab	Merck	IGF-1R	Inhibition of IGF/IGF-1R pathway	Phase II
Figitumumab	Pfizer	IGF-1R	Inhibition of IGF/IGF-1R pathway	Phase I
Cixutumumab	ImClone	IGF-1R	Inhibition of IGF/IGF-1R pathway	Phase II
Bevacizumab	Hoffman-La Roche	VEGF	Inhibition of angiogenesis	Phase II
Bisphosphonate				
Zoledronic acid	Merrion pharmaceuticals	Tumor microenvironment	Inhibition of bone resorption	Phase II
Phenolic compound				
Curcumin	Pharmanza Herbals	ABCB1	Inhibition of drug efflux	Phase I/II

Table 3: Targeted therapy for OS in clinical trial (Content extracted from Hattinger CM, Pasello M, Ferrari S. Emerging drug for high-grade osteosarcoma. Expert Opinion on Emerging Drugs 2010;15:4, 615-634. Table 2, Drugs and compounds of potential clinical interest that have entered or are presently included in the clinical trials for high-grade osteosarcoma; p. 621)

1.4. Canonical Wnt signaling pathway

The canonical Wnt signaling pathway plays a role in development by orchestrating cell differentiation, cell proliferation and cell fate determination. Activation of this pathway is associated with tumorigenesis (114). β-catenin is the central primary effector of this signaling pathway, in response to Wnt (Figure 5).

1.4.1. β-catenin*:*

(I) Structure

β-catenin is a 781 amino acid protein encoded by the CTNNB1 gene located on chromosome 3p21. Structurally, it is composed of three domains, each of which has sites for different binding partners and mediate different functions.

(i) N-terminal domain – Contains phosphorylation sites, Serine (Ser) 33, Ser 37, Threonine (Thr) 41, Ser 45 that are critically important for recognition and binding of β-TrCP ubiquitin ligase involved in the destruction of β-catenin (115).

(ii) Central armadillo domain – Comprised of 12 armadillo repeats, each of which has three α-helices (H1, H2, H3) densely packed giving it a cylindrical conformation. Several partners bind to this domain at different subcellular levels: α-catenin, E-cadherin bind at the cell membrane; axin, APC bind in the cytoplasm; and TCF/LEF, chibby, p300, ICAT, etc. in the nucleus. All binding ligands require a consensus sequence containing aspartic acid (Asp, D) and glutamic acid (Glu, G) which recognizes two residues of lysine (Lys) 435 & Lys 312 in the armadillo domain of β-catenin (115).

(iii) C-terminal domain – houses the transactivation domain required for gene activation.

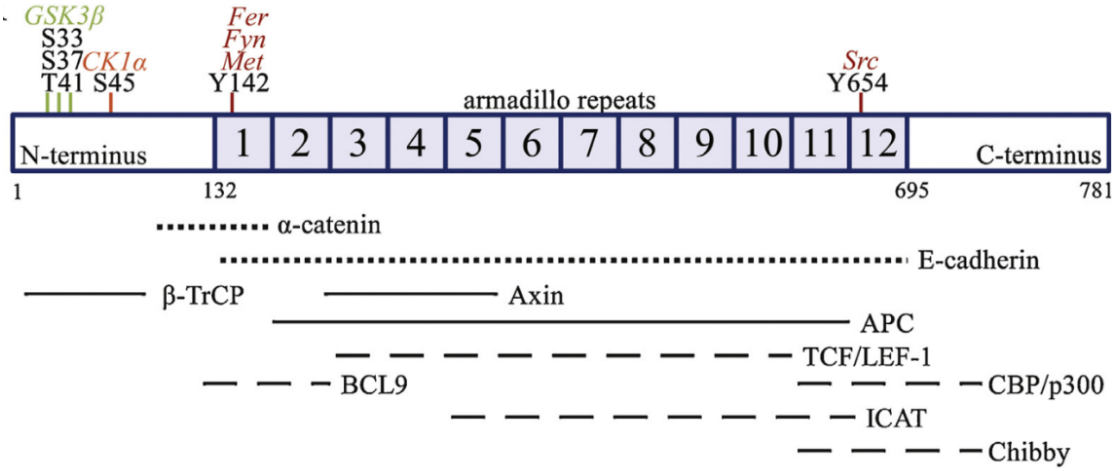

Figure 5: ***Structure of β-catenin***. β-catenin consists of three domains namely: N-terminal domain, Central armadillo domain and C-terminal domain. The N-terminal domain plays a key role in regulating the stability of β-catenin, the central armadillo domain helps in binding of other proteins to β-catenin and the C-terminal domain regulates the transactivation of β-catenin. Diagram adapted from Jamieson C, Sharma M, Henderson BR. Targeting the beta-catenin nuclear transport pathway in cancer. Seminars in cancer biology. 2014;27:20-9. Figure 2A, Schematic diagram of β-catenin protein with key serine (S), threonine (T) and tyrosine (Y) phosphorylation sites and protein interaction sites; p. 3.

(II) Role of β-catenin

β-catenin is a dual function protein that plays a role at the membrane in maintaining cell-cell adhesion and in the nucleus by promoting the transcriptional activity of TCF/LEF. Its function in the cell is dependent on the binding partners that associate with it.

(i) Adherens junction: At the cell membrane, β-catenin binds to E-cadherin (E-cad) and α-catenin, thereby indirectly modulating actin cytoskeleton. Binding to E-cad helps in maintaining cell-cell adhesion.

(ii) Nucleus: Inside the nucleus, β-catenin primarily binds to TCF/LEF transcription factor and promote the transcription of its downstream targets. Besides TCF/LEF, β-catenin also binds to a number of co-activators like p300, BCL9, Pygopus, SWI/SNF. Each of these co-activators promote the transcriptional activity by playing unique roles which will be discussed in the coming section (116).

1.4.2. Overview of Wnt-β-catenin signaling

β-catenin is constitutively formed in the cytoplasm, and its level is tightly regulated by a destruction complex which comprises of scaffolding proteins, axin, adenomatous polyposis coli (APC), kinases that phosphorylate β-catenin, glycogen synthase kinase 3 β (GSK3β), casein kinase I (CKI) and protein phosphatase 2A (PP2A). In the absence of Wnt signal, the free cytoplasmic β-catenin not bound to E-cad at membrane is degraded continuously by the destruction complex in a dual-kinase catalysed mechanism. The scaffolding proteins APC and axin interact with free cytoplasmic β-catenin and bind to its central domain, followed by which CKI and GSK 3β also get recruited to axin forming a multi-protein complex. In this complex, CKI phosphorylates β-catenin at Ser 45 at the N-terminal domain (NTD) which serves as a priming step for GSK 3β mediated phosphorylation at Ser 33, 37, Thr 41. β-catenin phosphorylated at Ser 37, Thr 41 is recognized by β-TrCP, a subunit of Skp, Cullin, F-box (SCF) ubiquitin ligase. Binding of SCF β-TrCP to β-catenin catalyzes polyubiquitination of β-catenin and its subsequent proteasomal degradation by the 26S proteasome. In the presence of Wnt signal, the ligand (Wnt) binds to its cognate receptor Frizzled (Fz) and co-receptor LRP6/5 (Low-density receptor-related protein) and recruits a cytoplasmic protein called Dishevelled (Dvl). Dvl further recruits the scaffolding protein of the destruction complex, axin along with GSK 3β, thereby disrupting the destruction complex. In the absence of a functional destruction complex, β-catenin formed in the cytoplasm accumulates and

eventually enters the nucleus. β-catenin lacks any classical nuclear localization signal (NLS) or nuclear export signal (NES) and, therefore, is thought to enter nucleus by direct interaction with the nuclear pore complex components like Nup358. Inside the nucleus, β-catenin binds to TCF/LEF transcription factor along with multiple co-activators such as BCL9/pygopus and subsequently displaces the TCF repressors Groucho/TLE. This displacement of the repressor, activates TCF and initiates the transcription of Wnt target genes. Many of the proteins translated from transcription of the Wnt target genes are involved in regulation of cell proliferation (c-myc), cell cycle regulation (cyclin D1), angiogenesis (VEGFA) and cell invasiveness (MMP). Therefore, unregulated over-expression of downstream targets of the Wnt pathway may support tumorigenesis. Hence, it is essential to maintain a tight control of transcription mediated by TCF/ β-catenin complex. The mechanism of deactivation of TCF/ β-catenin complex is poorly understood. One potential deactivation mechanism is a change in binding partners of β-catenin from activators to repressors. Chibby, one of the repressors deactivate TCF/ β-catenin by binding to the CTD of β-catenin. This binding blocks the co-activators bound to β-catenin and competes with TCF for β-catenin binding. Additionally, Chibby forms a tri-molecular complex with β-catenin and 14-3-3 protein which is exported out of the nucleus, effectively reducing nuclear β-catenin levels. The nuclear export of β-catenin may also be catalyzed by the sequestration of various components of destruction complex in the nucleus (116, 117).

Wnt signaling is primarily regulated by β-catenin and the role which β-catenin play relies on the type of post-translational modification of this protein. For example, phosphorylation on Ser37 and Thr41 provide a site for β-TrCP and targets β-catenin for destruction, whereas phosphorylation of Tyr142 reduces α-cat binding and impairs β-catenin's function at the adherens junction. Several such post-translational modifications of β-catenin and its regulatory function have been identified. Table 4 summarizes the currently known post-translational modifications of β-catenin and their regulatory functions.

MODIFICATION	SITES	ENZYME	FUNCTION (enhancement of)
Ser/Thr phosphorylation	S33, S37	GSK3	Degradation, provides sites for β-TrCP
	T41	GSK3	Degradation, phosporylation relay site
	S45	CK1	Degradation, priming for GSK3
	T112	CK2	Adhesion, promotes α-catenin binding
	T120	PKD1	Inhibition of signalling by immobilization of β-catenin in trans-Golgi
	S191	JNK2	Nuclear translocation
	S246	Cdk5	Inhibition of APC binding (via Pin 1)
	T393	CK2	Signalling, promotes stability
	S552	Akt, PKA	Signalling
	S605	JNK2	Nuclear translocation
	S675	PKA	Signalling, enhancement of CBP binding
	S675	PAK (p21 activ. kinase)	Signalling, promoting stability and transcription
	S23, S29	CK2 (?)	Stability (?)
	(?) (in *Drosophila*)	Hipk, HipK2	Promoting stability of Armadillo (opposite in other system reported)
	S764, S802, S827 (sites not in vertebrates)	NLK	Connecting Armadillo–E-cadherin complex with Wnt/PCP pathway
Tyr phosphorylation	Y654	Src	Signalling, reduces cadherin binding allows TBP binding
	Y142	Fer/Fyn; Met	Signalling, reduces α-catenin binding
	Y86, Y654	Bcr-Abl, Abl	Signalling, stabilizing β-catenin
	Y333	Src (EGFR mediated)	Signalling, promotes nuclear function in response to EGF (Wnt independent)
	Y489	Abl	Signalling, disrupts binding to N-cadherin
	Y654, Y670	Met (?)	Signalling, HFG-mediated release from membrane
Ubiquitylation	K19	SCF ubiquitin ligase	Degradation
	K666, K671	Siah-1	Degradation, block of signalling
Acetylation	K49	CBP	Signalling, enhancement of target specific β-catenin transcription *(c-myc)*
	K345	p300	Signalling, increases binding of TCF, reduces binding to AR

Table 4: Post-translational modifications of β-catenin. Diagram adapted from Valenta T, Hausmann G, Basler K. The many faces and functions of beta-catenin. The EMBO journal. 2012;31(12):2714-36. Figure 4B, Table summarizing possible translational modifications of β-catenin and their functional consequences; p. 2720.

1.4.3. Active β-catenin (ABC) – the transcriptionally active form of β-catenin

The stability and subsequent nuclear accumulation of β-catenin were conceived to be solely responsible for mediating β-catenin's function as transcriptional/trans-activator. However, a study by Staal *et.al.,* evolved this existing model by proposing that stability of β-catenin was insufficient for promoting β-catenin/TCF transcriptional activity. The study used two different systems that blocked β-catenin degradation, (i) a pharmacological proteasome inhibitor ALLN (N-acetyl-Leu-Leu-Norleu-al) and (ii) CHO cells harboring a temperature sensitive mutation in E1ubiquitin conjugation enzyme. In both cases, an accumulation of β-catenin occurred; however, the transcriptional activity of β-catenin /TCF remained unchanged. Additionally, a form of β-catenin that is unphosphorylated at Ser37 and Thr41 of the NTD was found to be expressed at elevated levels with Wnt1 stimulation and also promoted TCF transcriptional activity. Cumulatively, this study provided strong evidence for a partially unphosphorylated form (dephosphorylated on Ser37, Thr41) of β-catenin which is transcriptionally active, referred as Active β-catenin (ABC), to mediate Wnt signaling (118).

1.5. Wnt signaling in OS

Wnt signaling is known to play a role in bone development by regulating the cells involved in bone formation and remodeling. Wnt3a stimulates proliferation of mesenchymal stem cells (MSC) but suppresses differentiation, whereas Wnt10b promotes differentiation of MSC and triggerss osteoblastogenesis. The Wnt co-receptor, LRP5 is expressed by osteoblasts and helps in mediating Wnt signals for promoting proliferation and survival of osteoblasts, thereby influencing the construction of bone matrix. Negative regulators of Wnt signaling such as Dickkopf (Dkk) and Secreted frizzled-related proteins (SFRP) control bone formation and matrix density by regulating the levels of β-catenin. Wnt signaling also regulates osteoclast function primarily by mediating the transcription of downstream targets involved in osteoclastogenesis, RANKL and OPG. The role of Wnt signaling in bone remodeling hints at the possibility that deregulation of this pathway might lead to OS (119).

A number of studies have investigated the role of various components of Wnt signaling and have shown that deregulation of this pathway promotes OS. Increased expression of Wnt10b is observed

in patients with the metastatic condition and is associated with poor survival (120). The Wnt receptor LRP5, which is involved in mediating the signals for osteoblast proliferation in bone cells, is highly expressed in patients with high-grade OS (121). Additionally, knockdown of LRP using dominant negative LRP plasmid *in vitro* and *in vivo* has been shown to reduce expression of MMP2, MMP14 and decrease the metastatic potential of OS cells (122, 123). While these studies corroborate the role of Wnt signaling by positive regulators, few studies have also substantiated the involvement of Wnt signaling in OS by attenuating the pathway using inhibitors. The Wnt antagonist Wnt inhibitory factor (WIF) is epigenetically silenced in OS leading to increased β-catenin, promoting deregulated proliferation of osteoblasts and hence tumorigenesis of OS (124). WIF is shown to be downregulated in about 76% of OS cases and over-expression studies in animal models demonstrate the role of WIF in decreasing tumor growth rate and reducing lung metastasis. Dkk, another inhibitor of Wnt signaling, is also shown to play a role in OS by modulating invasiveness. Overexpression of Dkk-3 significantly reduces the invasive capacity of OS (125, 126). In contrast, Dkk-1 which is also a Wnt pathway inhibitor is shown to be maximally expressed in OS at the tumor periphery. It is thought that Dkk1 contributes to OS by preventing repair of surrounding osteoid as the tumor progresses (127). The above studies support a role of Wnt signaling in OS pathogenesis by modulating the pathway components. However, the role of β-catenin itself has only been investigated in a few studies, and its role in OS is controversial. While some of the studies propose β-catenin to promote OS progression, others suggest the contrary. Iwaya *et.al,* used an *in vitro* model of murine OS cell lines, Dunn cells and LM8 (a metastatic cell line derived from Dunn cells) to identify β-catenin expression in OS progression. This study showed increased cytoplasmic and nuclear expression of β-catenin in the metastatic LM8 cell line compared to Dunn cells. It also showed an increased cytoplasmic and nuclear expression of β-catenin in 5 patient samples with lung metastases (128). However, in contrast, Kidani *et.al,* showed over-expression of β-catenin in LM8 cells to result in loss of its metastatic potential. A study which carried out IHC (immunohistochemistry) on 47 OS patient samples showed positive nuclear/cytoplasmic β-catenin expression in 70% of cases (129), although it was later revealed by Ng *et.al.,* that only 3 among 47 cases showed nuclear staining of β-catenin (130). Lack of nuclear β-catenin was also supported by a study in which 52 OS patient samples and 4 OS cell lines were stained for β-catenin. All the cell lines and 90% of the biopsy samples were negative for nuclear β-catenin staining (131).

In summary, although it is established that Wnt signaling plays a role in OS pathogenesis, the role of its key regulatory protein β-catenin remains obscure. It is important to note that studies carried out for understanding the role of β-catenin in OS have focused on total β-catenin expression and not on the transcriptionally active form of β-catenin ABC, which is thought to be the important factor in mediating Wnt signal. In our current study we will focus on examining the involvement of ABC in OS progression.

1.6. Hypothesis

We hypothesize that ABC facilitates OS progression.

1.7. Objectives

(i) To identify the overall cellular expression of β-catenin and ABC in OS progression.
(ii) To identify the cytoplasmic/nuclear localization of β-catenin and ABC in OS progression.

Chapter 2.0
Materials and methods

2.0. Materials and Methods

2.1. Cell culture and transfection of plasmid constructs

We used two pairs of human OS cell lines; each pair represented OS progression and comprised of a parent OS cell line and a metastatic cell line derived from parent cell line: Pair 1) SaOS2 (parent cell line) and SaOS2-LM7 (metastatic cell line derived from parent SaOS2 cell line); Pair 2) HOS (parent cell line) and HOS-143B (metastatic cell line derived from parent HOS cell line). The SaOS2-LM7 cell line was derived by injecting SaOS2 cells into a nude mouse model. At 6 months after injection, the cells from lung metastases were isolated and reinjected into another mouse. This was repeated for 6 generations to acquire an aggressive, metastatic OS cell line SaOS2-LM7 (132). SaOS2-LM7 and its parent cell line SaOS2 were a gift from Dr. Eugenie Kleinerman's laboratory at The University of Texas, M.D. Anderson Cancer Center, USA. The HOS-143B cell line was derived by a Ki-Ras oncogenic transformation of HOS cell line (133). HOS (Catalog no. CRL-1543) and HOS-143B (Catalog no. CRL-8303) were purchased from ATCC. All cell lines were cultured in Minimal Essential Medium (MEM) (Catalog no. 11095-072, Gibco), supplemented with 10% fetal bovine serum (FBS) (Catalog no. 12483-020, Gibco) 1% penicillin-streptomycin (Catalog no. P0781, Invitrogen) , non-essential amino acids (NEAA) (Catalog no. 11140-050, Gibco) and 1mM sodium pyruvate (Catalog no. 11360-070, Gibco) at 37ºC and 95% O_2 and 5% CO_2.

2.2. Whole cell lysate preparation

At 90% confluence in 10 cm dishes, cells were washed twice with phosphate buffered saline (PBS) (Catalog no. SH30258.01, Thermo Scientific) followed by trypsinization using 0.25% trypsin-EDTA (Catalog no. 25200-056, Gibco) for two minutes at 37ºC. Cells were counted using a hemocytometer and $1x10^6$ cells were pelleted at 500 rpm in a centrifuge. 100 µl of RIPA lysis buffer (Catalog no. 20-188, Millipore) containing protease inhibitor cocktail (Catalog no. P8340, Sigma Aldrich) and phosphatase inhibitor cocktail (Catalog no. 524629, Millipore) was added to the pellet and the pellet was re-suspended by intermittent vortexing for 30 minutes. The re-suspended cells were placed on ice throughout the 30 minutes to avoid any degradation of proteins. The cell resuspensions were centrifuged in a micro-centrifuge at maximum speed for 5 minutes at 4ºC and supernatant was stored at -20 ºC.

2.3. Nuclear/cytoplasmic fraction isolation

The nuclear and cytoplasmic fractions were prepared using NE-PER nuclear/cytoplasmic extraction kit (Catalog no. 78833, Thermo Scientific) according to the manufacturer protocol using $1x10^6$ cells. The volume of each reagent that was used for isolation are; CER1 – 200 µl, CERII – 11µl, NER – 50 µl. In order to prevent contamination between fractions, a few steps of washes were incorporated into the protocol as suggested by the manufacturer. After collecting the cytoplasmic fraction, another spin for 1 minute at maximum speed was done and the supernatant cytoplasmic fraction was removed slowly using a pipette. The pellet was re-suspended (tap mixing) in 500 µl of ice cold PBS and centrifuged at 4ºC for 5 minutes at maximum speed in a micro-centrifuge. The supernatant was carefully removed using a vacuum pump and the pellet used for isolating the nuclear fraction according to manufacturer's protocol.

2.4. Western blotting

Sample preparation:

Whole cell lysate: Protein content in the whole cell lysate was quantified using BCA (Bicinchoninic acid) protein assay kit (Catalog no. 23227, Pierce). 40 µg of protein sample was boiled in 4X loading buffer for 5 minutes and then placed on ice for 5 minutes.

Nuclear/cytoplasmic fraction: 36 µl of each fraction was boiled with 4X loading buffer for 5 minutes and then placed on ice for 5 minutes.

Antibodies:

Following antibodies were purchased commercially and used at the indicated dilutions: β-catenin (Catalog no. 9587S, Cell signaling) 1:1000, Active β-catenin (Catalog no. 05-665, Millipore) 1:500, β-actin (Catalog no. sc69879, Santa Cruz) 1:10000, α/β-tubulin (Catalog no. 2148, Cell signaling) 1:1000, Lamin-B (Catalog no. MABE622) 1:1000, Anti-mouse IgG (Catalog no. NA934V, GE Healthcare), Anti-rabbit IgG (Catalog no. NA931V, GE Healthcare) 1:10000.

Western Blotting:

The prepared samples were run on a 7.5% SDS-PAGE and proteins were transferred to a polyvinylidene fluoride (PVDF) membrane (Catalog no. 1620177, Biorad) at 110 V for 70 minutes

at 4ºC. PVDF membranes were blocked for 1 hour using 5% non-fat dry milk powder in TBS (Tris buffered saline) containing 0.1% tween-20 (TBST) with constant shaking. Membranes were then incubated in primary antibody overnight at 4ºC and then washed 3 times in TBST for 10 minutes each. Membranes were then incubated in corresponding Horseradish peroxidase (HRP) linked secondary antibody for 1 hour at room temperature. After secondary antibody incubation, the blots were washed 3 times in TBST for 10 minutes each and visualized using SuperSignal West Femto (Catalog no. 34095, Thermo Fisher) or Western Lighting Plus ECL (Catalog no. NEL104001, Perkin Elmer)

2.5. Conditioned media concentration

Cells were grown to 80% confluence in 6 well plates, at which time complete media were replaced with 500ul serum free media and incubated for 24 hours. After 24 hours of incubation, the conditioned media were transferred to a fresh eppendorf tube and centrifuged for 1 minute at maximum 16000xg. The supernatant (media) were transferred to a Centricon filter (Catalog no. UFC501024, Millipore) and concentrated according to manufacturer's protocol. Briefly, 500ul of conditioned media were concentrated to approximately 50 µl by centrifugation for 10 minutes at 14000xg in a micro-centrifuge.

2.6. Gelatin zymography

10ul of the concentrated conditioned media in 6X loading buffer were loaded onto an 8% SDS-PAGE containing 2 mg/ml gelatin substrate (Catalog no. G8150, Sigma Aldrich). At completion of electrophoresis, gels were washed in 2.5% Triton X-100 v/v in water for 3 times, 20 minutes each. The washed gels were incubated overnight in incubation buffer (composed of NaCl, $CaCl_2$, Tris and NaN_3) at 37ºC and then stained with 0.05% Coomassie Brilliant Blue G-250 (Catalog no. B 1131, Sigma) for 2 hours. The gels were then de-stained using aqueous 4% methanol: 8% acetic acid. The gels were imaged using the Biorad Gel Doc apparatus and Quantity One software.

2.7. Densitometric analysis and statistical analysis

Western blots were quantified using the Image J software. Briefly, the bands of each protein to be quantified were chosen using a rectangular tool of identical size such that the same area was

analyzed for each band. This value corresponded to the intensity of signal from protein band. The intensity values of the protein of interest were normalized with the intensity values of the loading control (β-actin), to avoid any differences associated with loading. Statistical analysis was carried out by unpaired t-test using GraphPad Prism 6 software.

2.8. Immunofluorescence staining

Cells were cultured on coverslips to 30-40% confluence. Cells were briefly washed with PBS twice followed by incubation with 4% formaldehyde for 15 minutes at room temperature. Subsequently coverslips were incubated with 100% methanol at -20°C for 10 minutes for cell membrane permeabilization. Cells were blocked for 1 hour with 5% goat serum (Catalog no. 9023, Sigma Aldrich) in 1 PBS-Triton (0.3%) and then incubated with 1:200 anti-β-catenin antibody (Catalog no. 2677, Cell Signaling) or 1:200 anti-active- β-catenin diluted in blocking buffer overnight at 4°C. This was followed by incubation with AlexaFluor ® 555 goat anti-mouse antibody (Catalog no. A21422, Invitrogen) for visualization. Washes were carried out 3 times, 5 minutes each with PBS after fixation, permeabilization and primary antibody incubation. Subsequent to secondary antibody incubation, cell nuclei were stained with 300 nM 4', 6-diamidino-2-phenylindole (DAPI) for 7 minutes (Catalog no. D1360, Invitrogen). Coverslips were briefly rinsed with PBS and mounted on glass slide using Prolong antifade (Catalog no. P7481, Invitrogen). Cells were viewed at 40X magnification (oil immersion) using Carl Zeiss Laser Scanning Microscope and data were analyzed using LSM image browser software.

2.9. High content microscopy

High content microscopy was used to quantify the cellular expression of ABC and β-catenin after immunofluorescence staining. Cells were cultured in 96 well plate (Catalog no. 655090, Greiner Bio one) to 70% confluence. Cells were stained using the immunofluorescence protocol as described above. Images were taken at 20X magnification using ImageXpress Micro, Molecular Devices and analyzed using MetaXpress software. The MetaXpress software was used to perform a cell scoring analysis.

Cell scoring:

The cell scoring application module aids in identifying a sub-population of cells that are positive for a specific signal. In our experiment, the fluorescence signal from Alexafluor-555 was a measure of ABC or β-cat expression in cells. The software was used to detect two fluorescence signals (1) DAPI using DAPI channel and (2) Alexafluor-555 using Cy3 channel. The total number of cells were detected with nuclear staining by DAPI and the number of positive cells (ABC or β-catenin) were detected by the signal from Cy3 channel. We adopted this cell scoring module to determine the intensity of signal for ABC and β-catenin in different cell lines. Following are the steps that were involved in data acquisition and analysis using the MetaXpress software with pictorial representation. Configuration settings were carried out by defining the cell and nuclear area, to enable the software analyze the intensity of signal in the defined area. In order to ensure quantification of the actual signal of ABC or β-catenin, the area chosen for detection was defined stringently. Inclusion of any background area which would cause false intensity values was rigorously avoided (Figure 8, 9 & 10). Once the configurations were set, the software analysis provided various measurements such as cell area, cell average intensity, cell integrated intensity etc (Figure 11). We used average cell intensity and average nuclear intensity values for our analysis.

Average intensity = Integrated intensity of signal from pixels/number of pixels

Since the sum of intensity of signal from each pixel is normalized to the total number of pixels in the image of cells, average intensity values are comparable between cell lines.

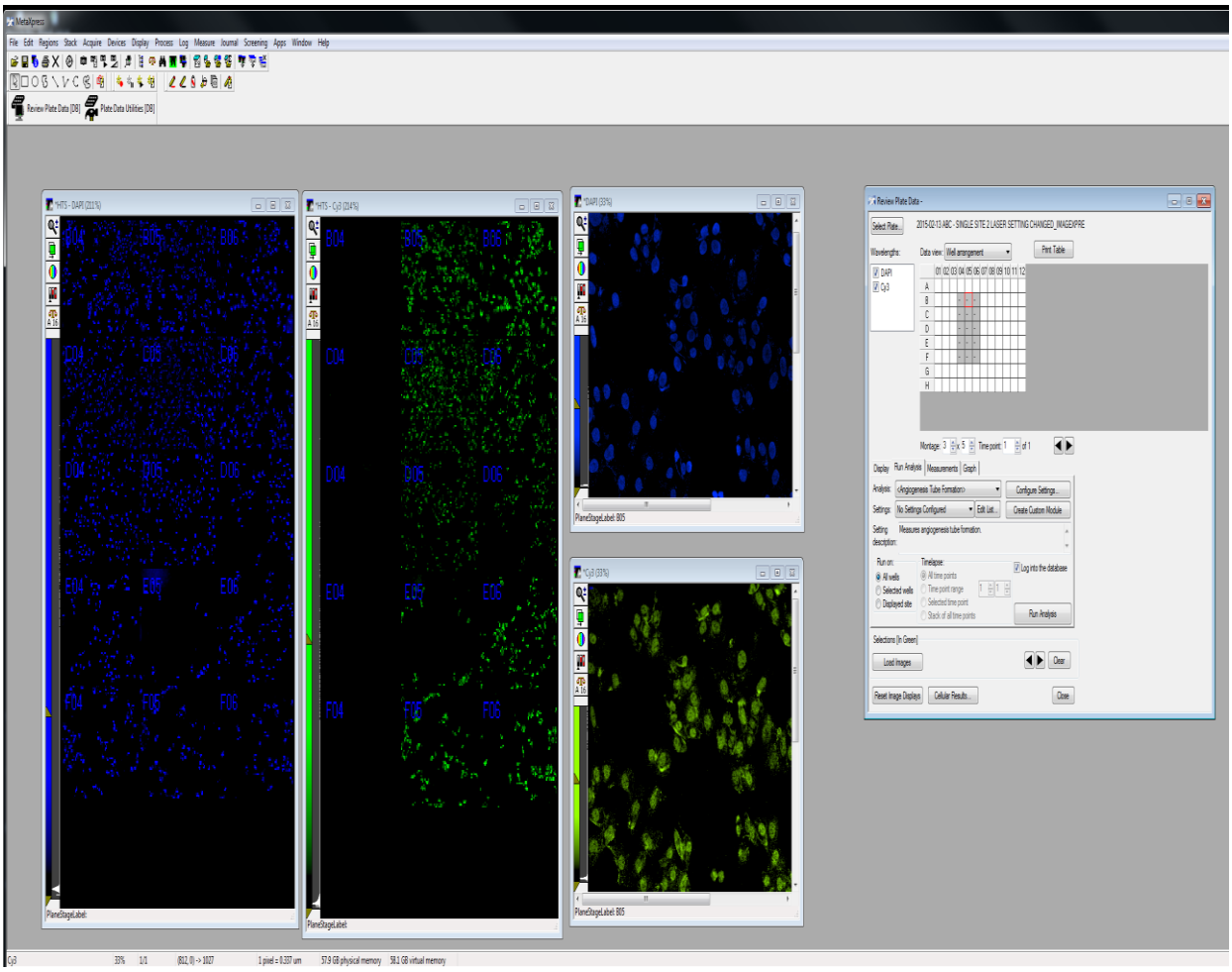

Figure 6: ***Screenshot of the work panel in MetaXpress software*:** Acquired images of cells from all wells. Nuclear staining, DAPI channel (Blue) and Cy3 channel for ABC expression (Green).

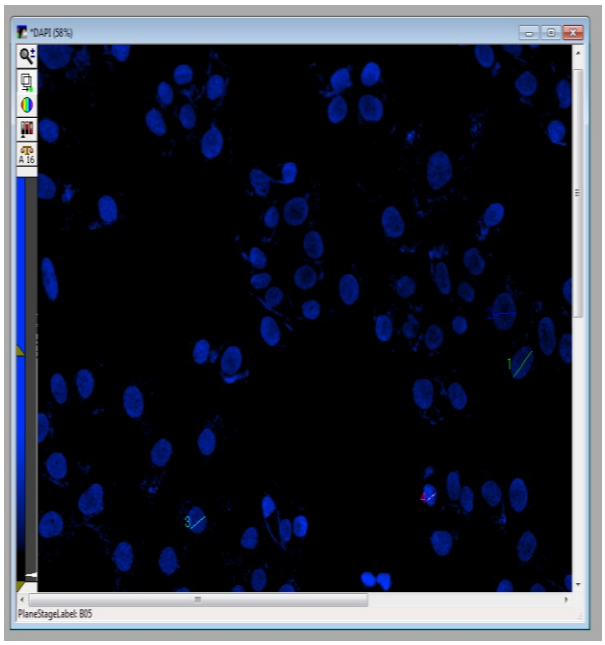

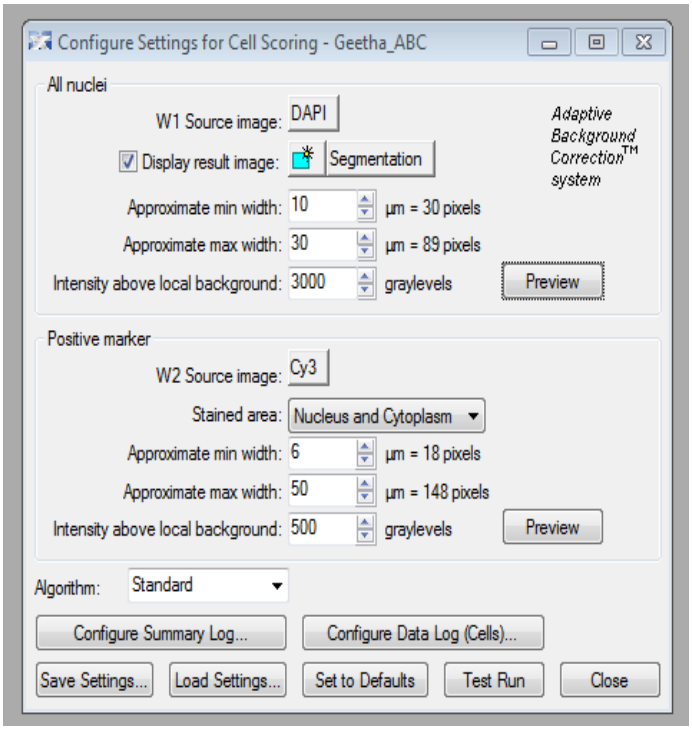

Figure 7: ***Configuration settings for cell scoring*****:** The boundaries of cells and nuclei were demarcated in order to cover the actual area of staining without inclusion of background. This was done by providing the width and minimum intensity of signal from cells and nuclei. This screenshot shows the settings that were followed for DAPI channel.

β-catenin 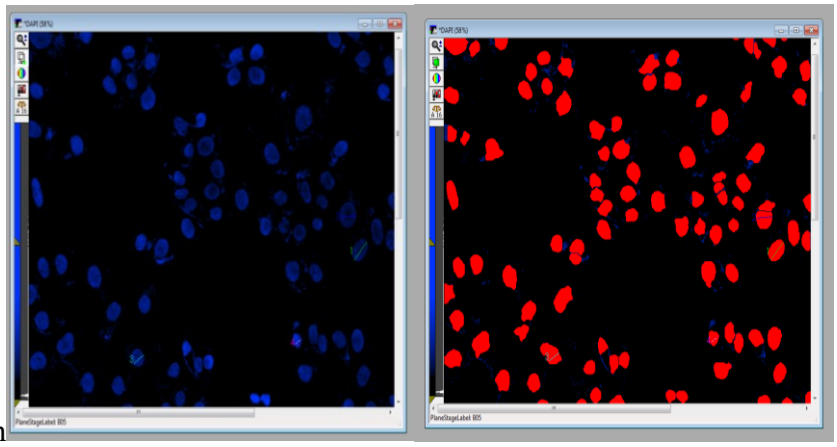

Figure 8: ***Preview of configuration settings for DAPI channel****:* The image on the left (blue) shows the DAPI staining for cells in a well. The image on the right (red) shows the area coverage by nuclei based on set configurations. Note that the area of nuclei by DAPI signal (blue) and the area covered by software for analysis (red) are close, indicating the stringency in setting the nuclear boundary.

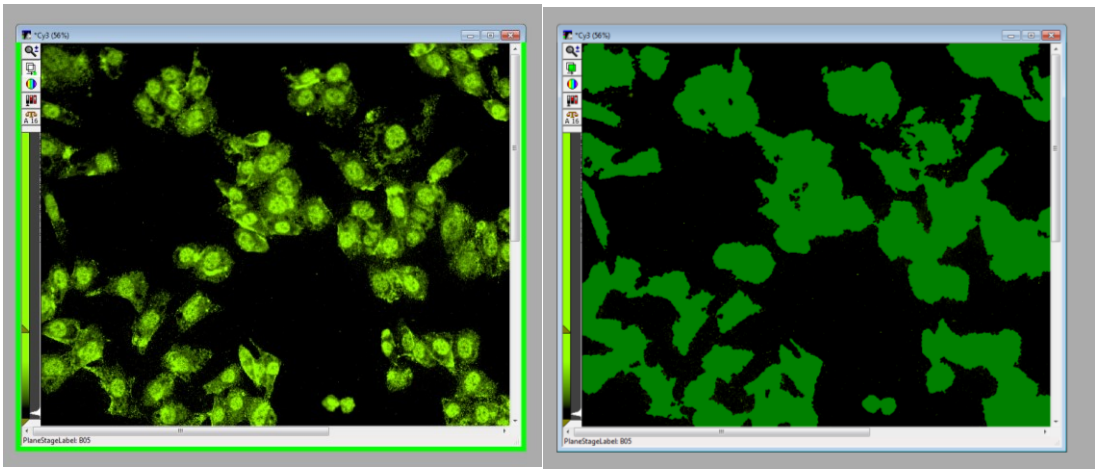

Figure 9: ***Preview of configuration settings for Cy3 channel:*** The image on the left (green) shows the ABC staining for cells in a well. The image on the right (dark green) shows the area coverage by ABC signal based on set configurations. This area was analyzed for intensity of signal by software. Note that the area of cellular ABC signal from Cy3 signal (green) and the area covered by software for analysis (Dark green) are close.

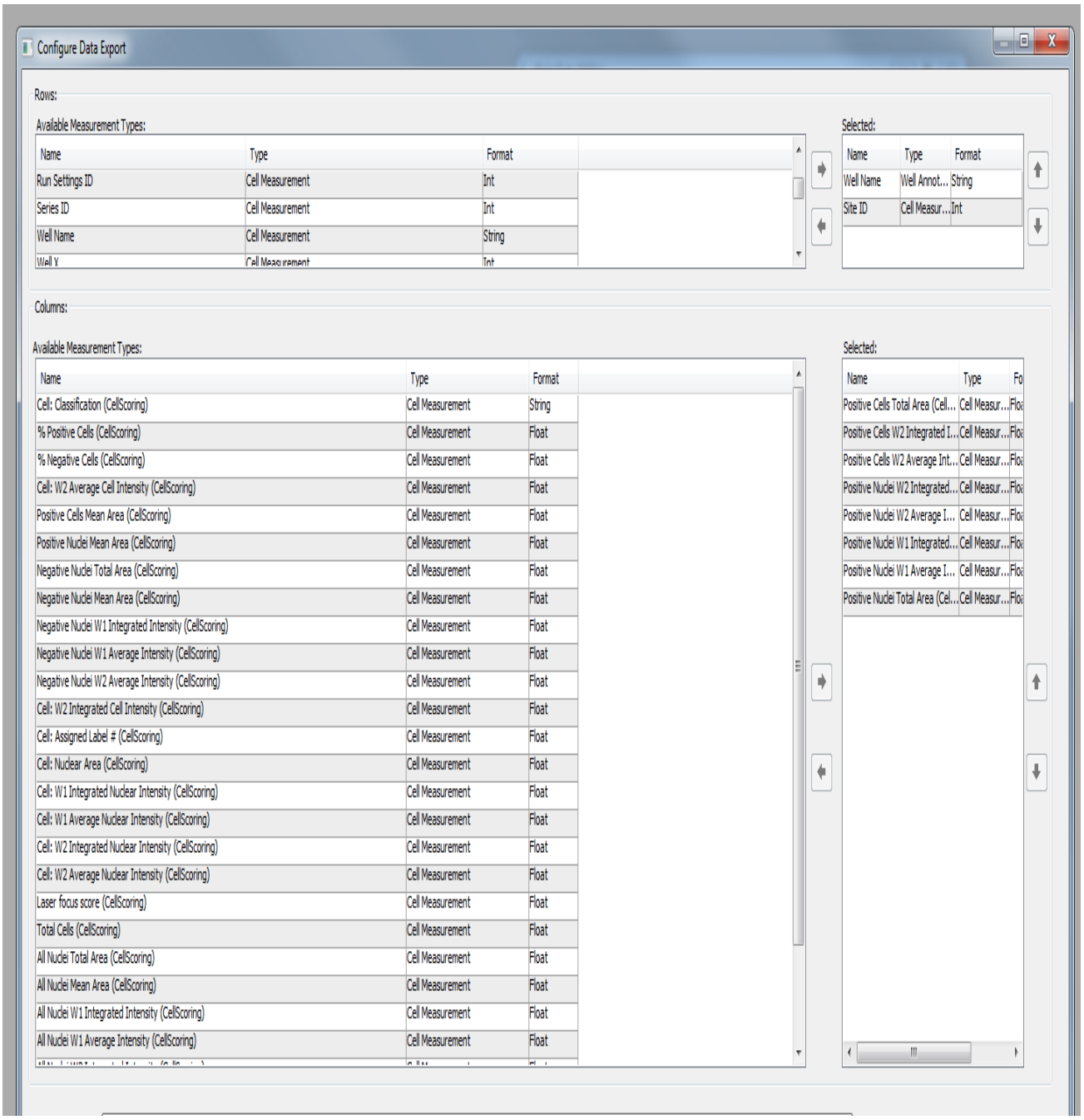

Figure 10: ***Measurements provided by software after analysis***.

Chapter 3.0
Results

3.0. Results

3.1. MMP activity increases with metastatic potential in cell lines

Since we intended to study the role of β-catenin and ABC in OS progression, it was essential to confirm the presence of indicator of metastatic potential of cell lines used in the study. Based on the literature, it is known that SaOS2-LM7 and HOS-143B are metastatic compared to their respective parent cell lines SaOS2 and HOS. However, we confirmed the metastatic potential of the cell lines using two of the currently known OS specific markers namely MMP2 and MMP9.

MMP2 and MMP9 are gelatinases which are implicated in cancer by their ability to remodel the extracellular matrix, promoting invasiveness. These gelatinases are formed in cells as a pro-enzymes, also known as zymogens. The latency of these gelatinases is maintained by the binding of their pro-domains to the catalytic domains of the MMPs, thereby shielding their active sites and inhibiting the enzyme activity. The pro-enzyme is activated at the cell membrane by the interaction between membrane type metalloproteinase (MT1-MMP), Tissue inhibitor of metalloproteinases (TIMP2) and MMP2/9. At the cell membrane, TIMP2 binds to active MT1-MMP and this MT1-MMP-TIMP2 complex recruits pro-MMP2 or 9, then cleaves the pro-domain of MMP2 or 9, thereby forming active MMP2 or 9 (134). Although the pro-enzyme form of MMP is physiologically inactive, its activity is observed on the gelatin zymography. The MMP activity by the inactive form on zymography, is due to the unfolding of latent form to catalytically active form by SDS that is used in zymography (135).

We determined the activities of MMP2 and MMP9, in the two paired cell lines used in this study, by gelatin zymography. Our results showed that there was no significant difference in the levels of the proenzyme form of MMP2 in either pair of cell lines. However, the gelatinase activity of the active (cleaved) form of MMP2 was significantly increased in SaOS2-LM7 compared to the parental SaOS2 cell line; there was negligible activity of the cleaved MMP2 in SaOS2 cells (Figure 11A). On the other hand, no cleaved MMP2 activity was detected in the HOS and HOS-143B cell lines. However, the HOS-143B cells exhibited greater MMP9 activity compared to HOS (Figure 11B). The MMP activities were consistent with the greater metastatic phenotype of the SaOS2-LM7 and HOS-143B cells compared to their respective parental lines, and supported the use of the two pairs of cell lines: pair 1) SaOS2 / SaOS2-LM7 and pair 2) HOS / HOS-143B as model systems representing OS progression.

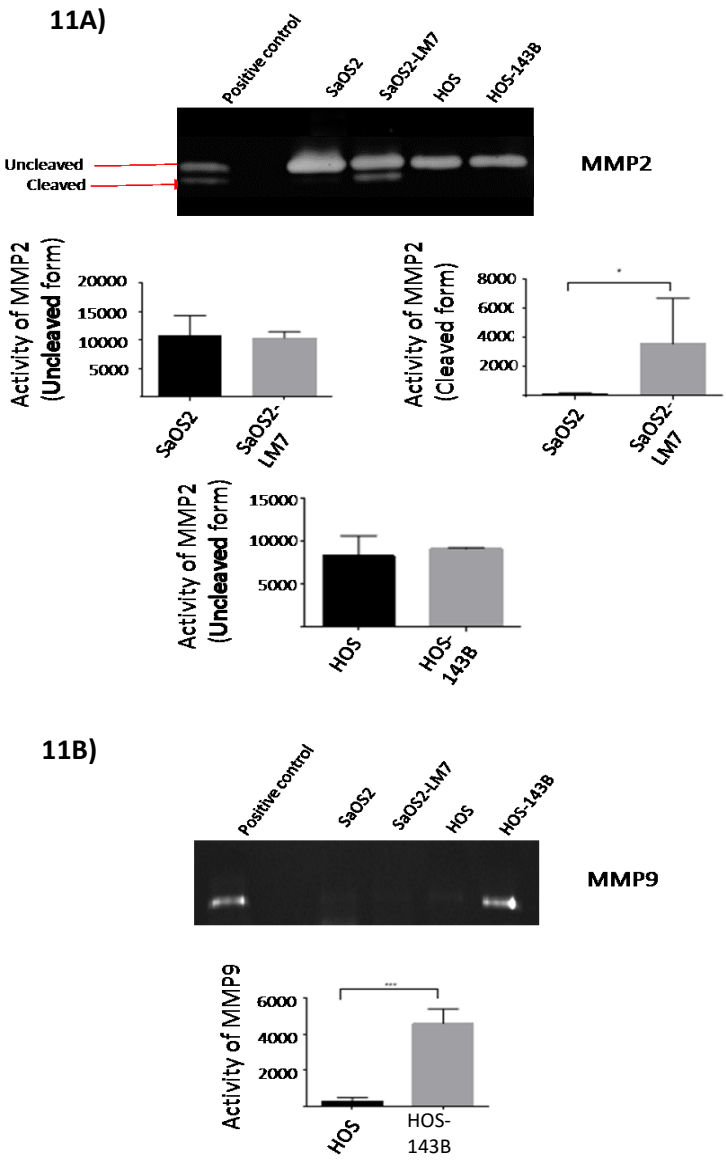

Figure 11: ***Metastatic potential of OS cell lines*.** Gelatin zymography for A) MMP2 B) MMP9, using concentrated conditioned media from cells grown in serum free media for 24 h, conditioned media from HT1080 cell line were used as positive control. No significant change was observed in the uncleaved form of MMP2 in both pairs of cell lines. However a significant increase was observed in the activity of cleaved (active) MMP2 in SaOS2-LM7 compared to SaOS2 n=5, *$p<0.05$. Although HOS/143B did not show any activity of cleaved MMP2, it showed a significantly increased MMP9 activity in HOS-143B compared to HOS n=3, ***$p<0.001$.

3.2. Cellular level of ABC is increased with OS progression

We next determined the cellular levels of β-catenin and ABC in the two paired cell lines, in order to see if there were any differences in their levels with OS progression. Cellular levels of β-catenin and ABC were determined in whole cell lysates of the paired cell lines using Western blot analysis. As shown in Figure 12A, both SaOS2-LM7 and HOS-143B showed increased total cellular levels of ABC compared to their parent cell lines SaOS2 and HOS. However, no significant differences in the cellular levels of total β-catenin was observed (Figure 12B). These results suggest that cellular ABC levels, specifically, are associated with OS progression.

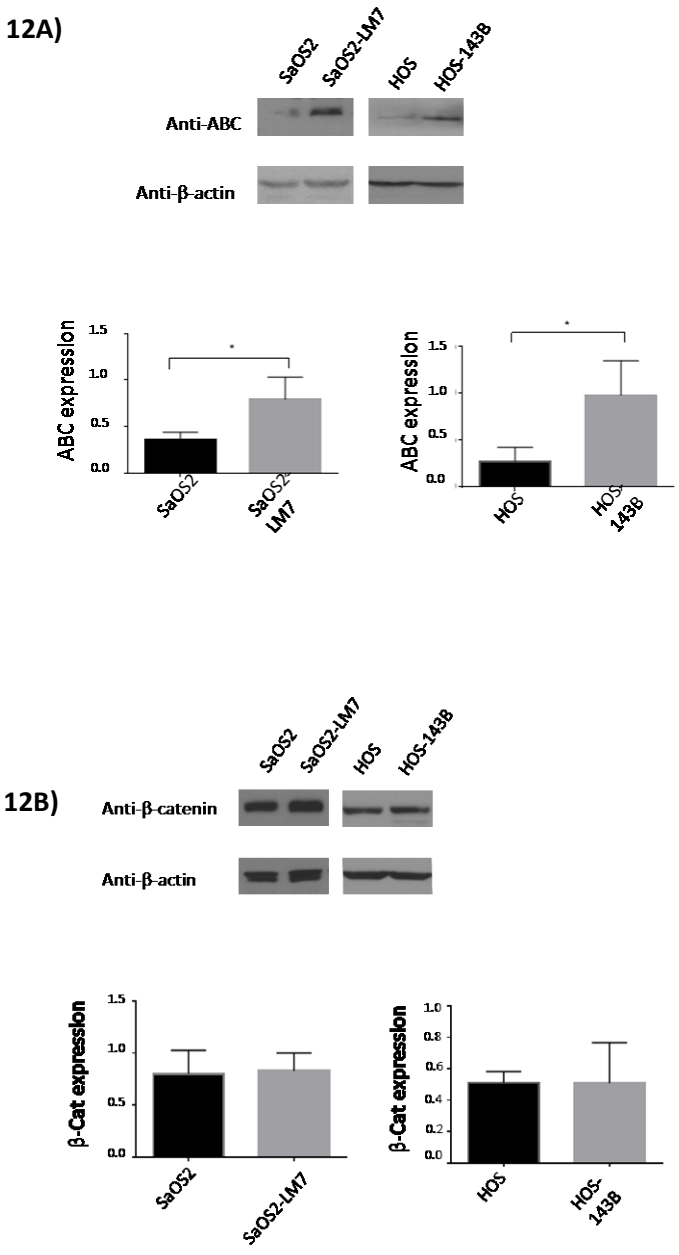

Figure 12: ***Cellular levels of ABC increases with OS progression***. Western blot analysis of A) total ABC level and B) total β-catenin level in whole cell lysates of OS cell lines. The cellular levels of ABC were increased significantly in the metastatic cell lines (SaOS2-LM7, HOS-143B) compared to their less aggressive parent cell lines (SaOS2, HOS) n=3, *$p<0.05$. However no differences in the cellular levels of β-catenin was observed with progression. Blots represented are from one experiment and the graphs are representative of three experiments.

3.3. Increased nuclear level of ABC with OS progression in SaOS2 / SaOS2-LM7 pair of cell lines

Since β-catenin and ABC shuttle between cytoplasm and nucleus, and their oncogenic role is mainly associated with their presence in the nucleus, we determined the levels of β-catenin and ABC in the cytoplasmic and nuclear fractions of the two paired cell lines. Using Western blot analysis, we found that there were significantly higher levels of ABC in the nuclear fraction of SaOS2-LM7 compared to SaOS2. However, there was no difference in the cytoplasmic levels of ABC between these two cell lines (Figure 13A). β-catenin levels were similar in both nuclear and cytoplasmic fractions of SaOS2 and SaOS2-LM7. α/β tubulin and Lamin B were used as cytoplasmic and nuclear markers, respectively.

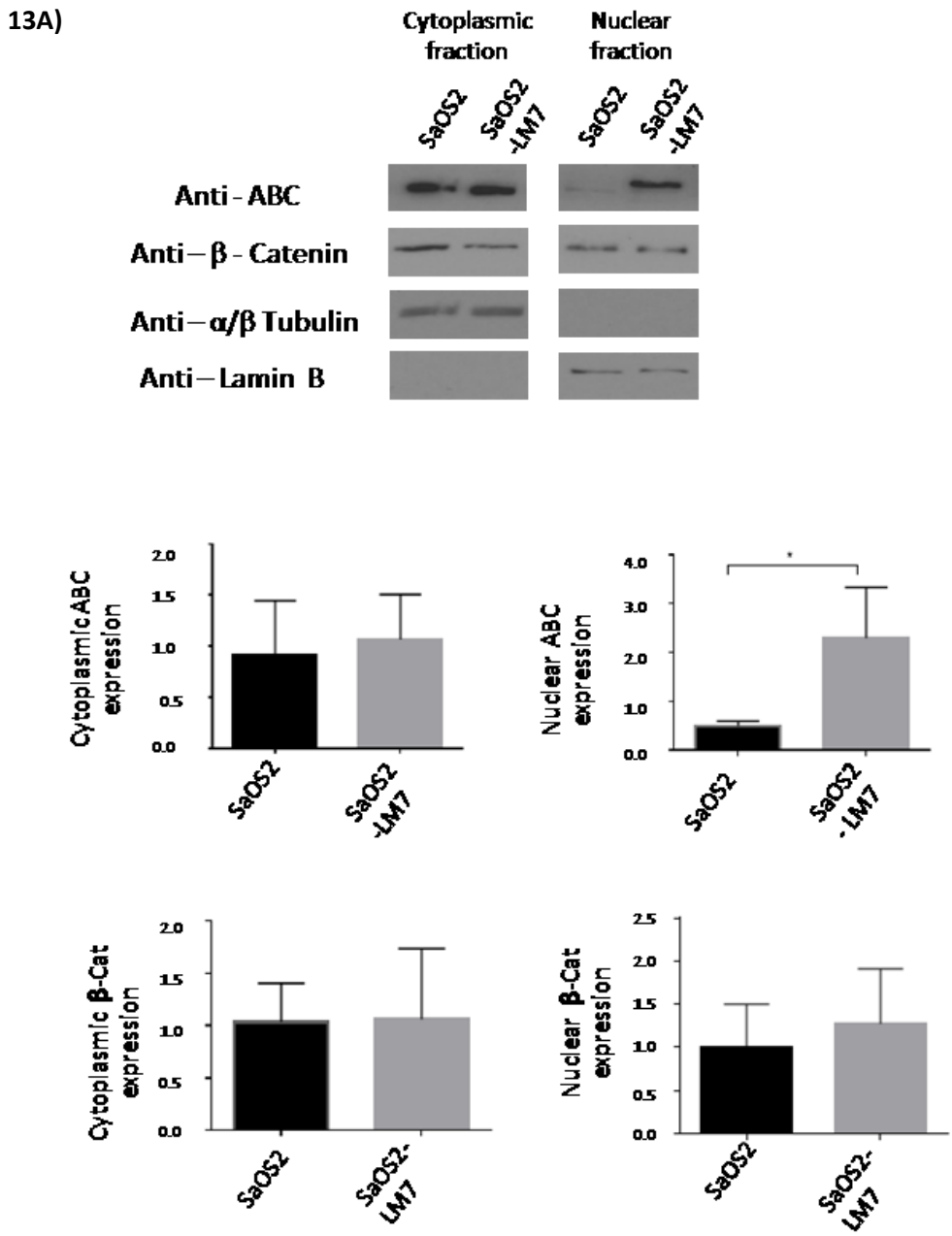

Figure 13A: ***Increased nuclear levels of ABC in LM7 compared to SaOS2.*** Western blot analysis for ABC and β-catenin in cytoplasmic and nuclear fractions. Nuclear ABC levels were significantly higher in LM7 compared to SaOS2 n=3, *$p<0.05$. However no differences in the levels of cytoplasmic ABC, cytoplasmic β-catenin and nuclear β-catenin were observed. Blots represented are from one experiment and the graphs are representative of three experiments.

3.4. Stable nuclear and cytoplasmic levels of β-catenin and ABC in HOS/HOS-143B pair of cell lines

Western blot analysis for cytoplasmic and nuclear fractions of HOS and HOS-143B did not show any definitive changes in the levels of ABC or β-catenin between the cell lines. Figure 13B is representative of three experiments. α/β tubulin and Lamin B were used as cytoplasmic and nuclear markers, respectively. Among these experiments, the trend for nuclear ABC level in the cell lines have been different between experiments. The available number of repeats for this experiment were insufficient to draw a conclusion.

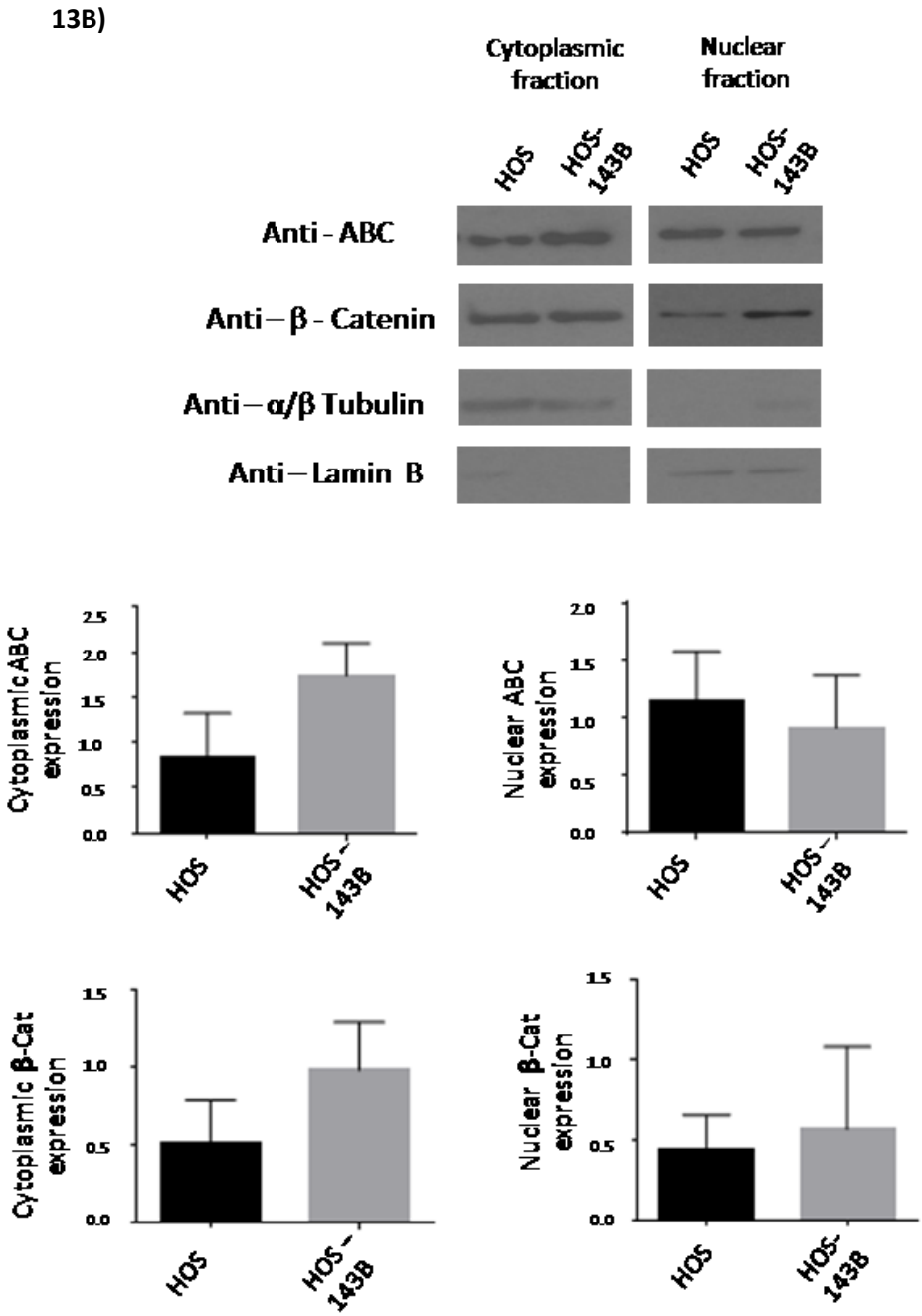

Figure 13B: ***Increased cytoplasmic levels of ABC in HOS-143B compared to HOS***. Western blot analysis for ABC and β-catenin in cytoplasmic and nuclear fractions. Cytoplasmic ABC level showed a trend to be higher in HOS-143B compared to HOS. However this change was not not significant n=3, *p=0.06. There was no significant alterations observed in the levels of nuclear ABC, cytoplasmic β-catenin and nuclear β-catenin. Blots are representative from one experiment and the graphs are representative of three experiments.

3.5. Increased nuclear localization of ABC with OS progression in SaOS2 / SaOS2-LM7

While the levels of ABC and β-catenin in the nuclear and cytoplasmic fractions were determined by Western blot analysis, the cellular localizations of β-catenin and ABC were determined with immunofluorescence microscopy. As shown in Figure 14A, there were higher levels of ABC localized predominantly in the nucleus for SaOS2-LM7 cells compared to its parental SaOS2 cell line. In contrast to ABC localization, β-catenin showed strong membrane localization but did not show any difference in the nuclear and cytoplasmic localization for SaOS2 and SaOS2-LM7 cell lines. Hence, the immunofluorescence images were in concordance with the Western blot analysis for cytoplasmic and nuclear fractions.

14A)

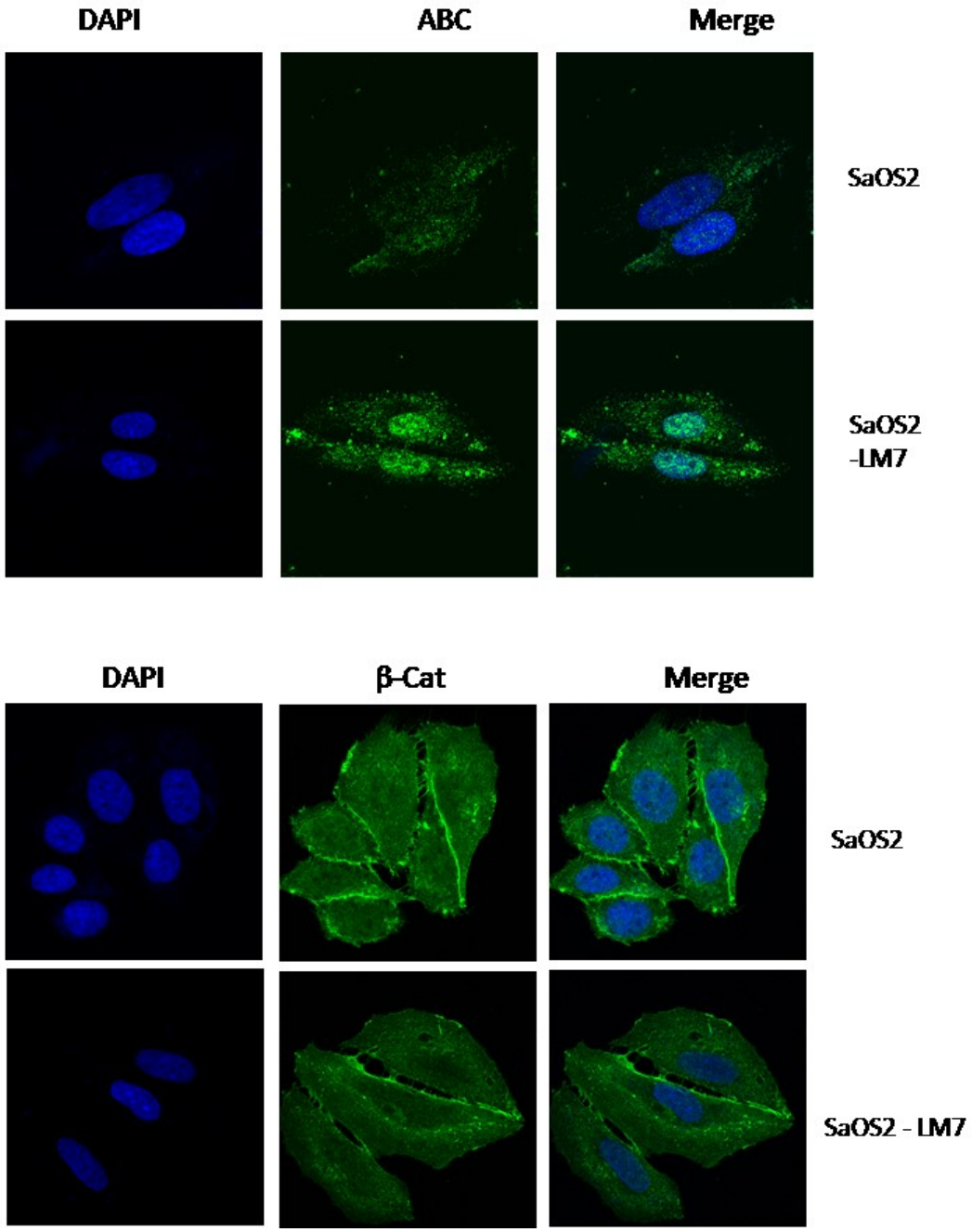

Figure 14A: ***Cellular localization of ABC and β-catenin in SaOS2 and SaOS2-LM7.*** Immunofluorescence analysis for ABC in SaOS2 and LM7 shows a predominant localization of ABC in nuclear area for SaOS2-LM7 compared to SaOS2. There was no difference in β-catenin cellular localization pattern in both cell lines. Images are representative of 3 experiments.

3.6. Increased nuclear localization of ABC with OS progression in HOS / HOS-143B

The immunofluorescence analysis of HOS and HOS-143B showed increased nuclear localization of ABC in HOS-143B compared to HOS. However, no specific difference in the cellular localization of β-catenin was observed between HOS and HOS-143B cell lines (Figure 14B). The observation from immunofluorescence staining of ABC was different from the findings in western blot analysis of nuclear and cytoplasmic fractions.

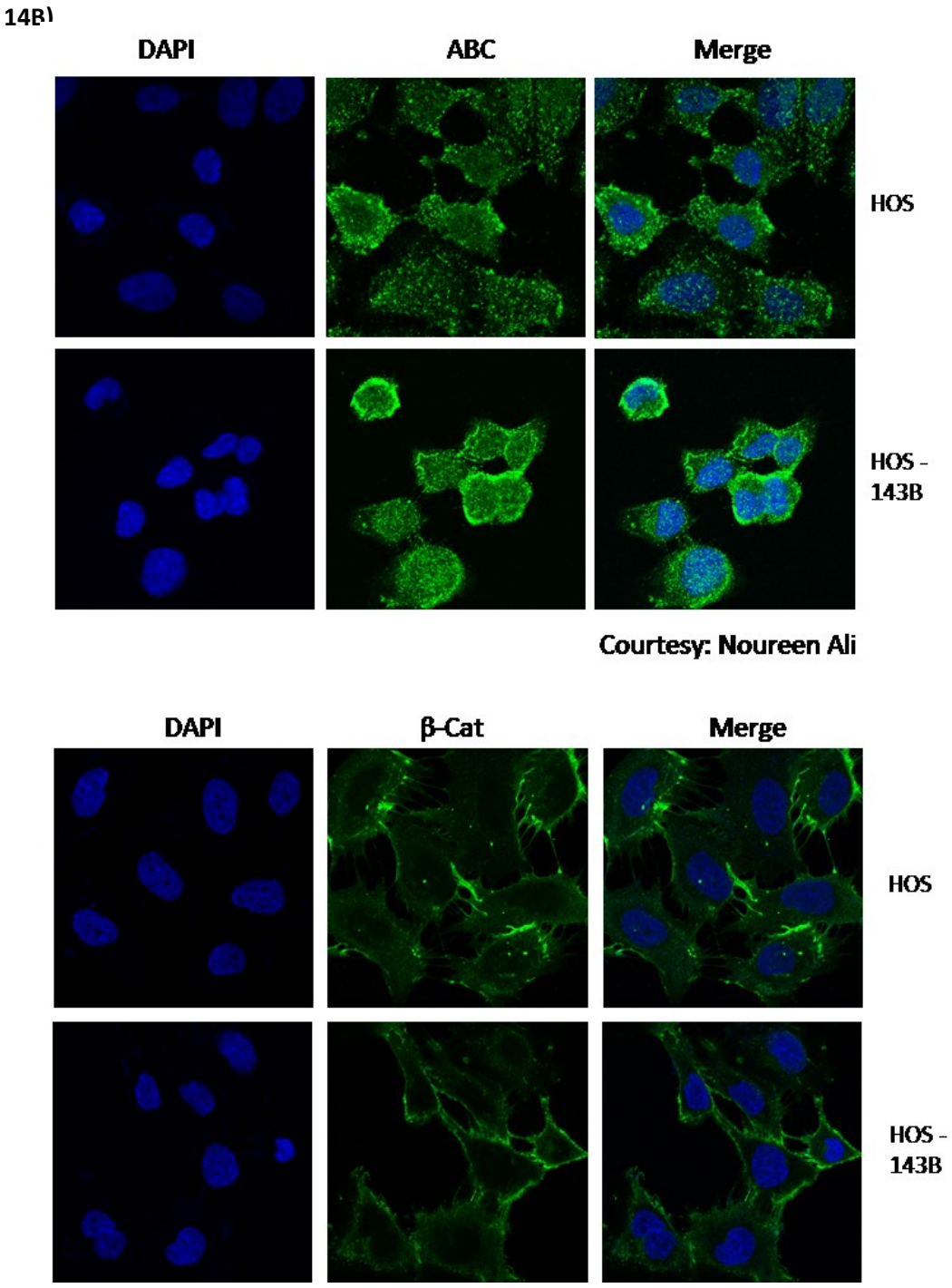

Figure 14B: ***Cellular localization of ABC and β-catenin in HOS and HOS-143B***. Immunofluorescence analysis showed increased nuclear localization of ABC in HOS-143B cell line compared to HOS. No difference in the cellular localization of β-catenin was observed between the cell lines. Images are representative of 2 experiments for ABC staining and 3 experiments for β-catenin staining.

3.7. High content microscopy shows increased nuclear ABC with OS progression in HOS/HOS-143B

Although the western blot analysis on nuclear and cytoplasmic fractions for HOS/HOS-143B pair of cell lines showed inconclusive results, immunofluorescence staining showed an increased nuclear ABC in HOS-143B compared to HOS. In order to confirm the immunofluorescence imaging results for HOS and HOS-143B cell lines, we used high content microscopy technique to quantify the immunofluorescence signal for ABC. The cellular and nuclear intensities of ABC signal were calculated using the MetaXpress software. We observed that the total cell intensity of ABC was increased with OS progression, which was in concordance with the results from Western blot analysis of whole cell lysate. On the other hand, the nuclear intensity of ABC was significantly increased in HOS-143B compared to HOS, which was in concordance with the observations from immunofluorescence images (Figure 15).

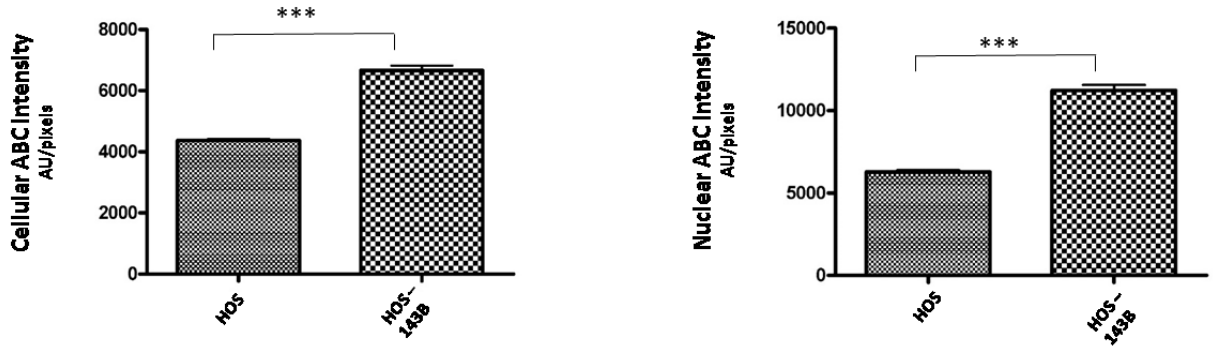

Figure 15: ***Quantification of ABC intensity using high content microscopy***. Immunofluorescence images from high content microscopy were quantified using MetaXpress software for cellular intensity and nuclear intensity. Analysis showed an increase in the cellular and nuclear intensities of ABC with OS progression in HOS/HOS-143B pair of cell lines. The statistical analysis was performed on the average intensity values for approximately 200 cells in each cell line. $p<0.0001$

Chapter 4.0
Discussion

4.0. Discussion

Osteosarcoma is a malignancy of the bone that occurs with the highest prevalence in children and adolescents. Currently, surgery with adjuvant chemotherapy is widely used for treatment of primary OS. The advent of adjuvant chemotherapy with multiple chemotherapeutic drugs has aided in performing limb salvage surgery (136) which preserves the function of limb. Although chemotherapy has proven to be effective in treating primary tumors, there are several long-term adverse effects associated with this treatment. These include renal and blood disorders (38, 137), cardiac disorders (138) and the genesis of a second tumor (139). Since OS is a pediatric cancer that occurs in the early life, it is crucial to ensure the quality of life of the patient in addition to effective elimination of tumor for improved survival. Therefore, considering the adverse effects associated with chemotherapy, especially with multi-agent chemotherapy and intensified dosage of chemotherapeutic drugs on a long-term basis, it is of utmost importance to modulate the administration of chemotherapy according to the aggressiveness of OS tumor. Stratification of patients based on the aggressiveness of tumor should benefit administration of optimal treatment on a case by case basis. In order to stratify the patients for treatment, prognostic markers predictive of the disease course is of pivotal importance. Currently available clinical prognosis for OS is based on factors such as stage of disease (140, 141), tumor size (142), local recurrence (143, 144), metastasis (141), and response to chemotherapy (145, 146). These prognostic factors are certainly of importance but, are only apparent in the later stage of the disease course (147). Therefore, identification of molecular markers that serves as an indicator of OS progression will potentially aid clinicians in assessment of disease course and plan optimal treatment regimens appropriately.

Further, while the existing treatment modalities have improved the disease free survival rate to 70% for patients with primary tumor, it still remains ineffective (25% - 30%) for patients presenting with metastatic disease. Also, it has been reported that change of chemotherapeutic drug or intensification of dose may not be useful in salvaging poor responders (148). Therefore, it is essential for the development of new therapeutic strategies aimed at improving the survival of OS patients.

Understanding the biology of OS progression is of key importance in identifying biomarkers with prognostic value and targets for improved therapy. Accordingly, in this study, we investigated the Wnt signaling pathway that is well known to play an integral role in bone development and therefore anticipated to play a role in OS pathobiology. Specifically, we focused on understanding the role of β-catenin and ABC, two central proteins in the activity of the Wnt signaling pathway, in OS progression.

While previous studies have shown that the Wnt signaling pathway plays a role in mediating OS progression, the role of β-catenin itself remains unclear. There are mixed contradictory reports with respect to the role of β-catenin in OS progression: while some studies support the role of β-catenin in OS progression, there are other studies that do not. However, all studies carried out to date have focused on β-catenin rather than its transcriptionally active form, Active Beta Catenin or ABC. We investigated the role of ABC and β-catenin in OS progression. Our study highlighted that, while ABC was associated with OS progression, β-catenin itself was not involved. To the best of our knowledge this is the first study that has reported the potential role of ABC in OS progression.

In this study, we used an *in-vitro* model comprised of two pairs of OS cell lines representative of OS progression. The first pair of cell line was SaOS2 (parent cell line) and SaOS2-LM7 (metastatic cell line). The other pair of cell line used was HOS (parent cell line) and HOS-143B (metastatic cell line). The 143B cell line was shown to have the highest metastatic potential in a study which characterized a number of OS cell lines by injecting into mice (149). A study from Flores *et.al.* predicted the metastatic pathways that are involved in OS based on the genomic and proteomic profiles of these cell lines. This study summarizes the various genetic changes in these two pairs of cell lines (150).

We confirmed expression of markers of metastatic potential of these cell lines by determining the levels of MMP2 and MMP9 (89-92). MMPs are gelatinases secreted from cells that degrade extracellular matrix compounds. MMPs secreted by tumor cells play an important role in

promoting invasiveness and aid the metastasis process. Therefore, we used gelatin zymography to determine the activities of secreted MMP2 and MMP9 from conditioned media of the cell lines. We observed that MMP activity was increased in the metastatic cell lines compared to the parental cell lines. Specifically, activity of cleaved MMP2 was increased in SaOS2-LM7 compared to its parent cell line SaOS2, whereas MMP9 activity was increased in HOS-143B compared to its parent cell line HOS (Figure 12). Collectively, the gelatin zymography data suggested the increased metastatic potential of HOS-143B and SaOS2-LM7 cell lines compared to their respective parent cell lines *in-vitro*.

We determined the cellular levels and localization of β-catenin and ABC in OS cell lines. Our results showed that the cellular levels of ABC were increased with OS progression, there was no alteration in the cellular level of total β-catenin with OS progression (Figure 13).β-catenin In addition to this, the sub-cellular localization studies for ABC showed increased nuclear accumulation of ABC in the metastatic cell lines compared to their respective parent cell lines (Figures 14A, 15A, 15B and 16) . On the other hand, cellular localization of β-catenin was unaltered with progression in both pairs of cell lines; the nuclear/cytoplasmic levels of β-catenin and its cellular localization were unchanged with progression (Figures 14A, 15A, 15B).

Previous studies have investigated the cellular localization of β-catenin in OS, using cell lines or tissue samples. A study by Iwaya *et.al,* reported increased nuclear and cytoplasmic β-catenin to be associated with OS progression using a murine model (128). In this study, two murine OS cell lines, the Dunn cells and its metastatic variant cell line LM8 cells were used. Both cell lines were injected into mice and analyzed for β-catenin localization using immunohistochemistry. An increased expression of β-catenin at the invasive front was observed in the mice injected with metastatic cell line LM8, compared to those injected with Dunn cells. Hence, the study suggested β-catenin was associated with OS invasiveness. Interestingly, in contrast to this study, Kidani *et.al.* showed an increased cellular expression of β-catenin to be associated with reduced metastatic potential in same LM8 cells (151). Therefore, the association of increased β-catenin with OS progression remains inconclusive in murine models. Studies with human OS cell lines or tissue samples to investigate the association of β-catenin with OS progression are also not conclusive.

Iwaya *et.al,* reported nuclear and cytoplasmic expression of β-catenin by carrying out immunohistochemical staining on 5 metastatic OS patient samples. However, there were no primary tumor control tissues used in the study and therefore it lacks support for the differential expression of β-catenin with OS metastasis (128). Another study carried out IHC for β-catenin on 47 patient samples and evaluated the correlation between β-catenin staining and clinico-pathologic data available for these tissues. 33 of the 47 patients showed positive staining for β-catenin (129). However, only 3 of the cases exhibited prominent nuclear β-catenin (130). Further, there was no correlation between the β-catenin levels and clinicopathologic data. Cumulatively, these studies indicate that while β-catenin expression is evident in OS, it is likely not differentially expressed with OS progression.

Our results show β-catenin level and cellular localization to be unchanged with OS progression, which is in concordance with the findings from existing studies (129-131). Our observations regarding the cellular localization pattern of β-catenin immunofluorescence imaging were similar to those shown by Cai *et.al.* (131), supporting the notion that total β-catenin may not be differentially expressed or localized with OS progression. Therefore, β-catenin may not be a worthy prognostic marker for OS. On the other hand, our study demonstrated an association of ABC with OS progression *in vitro*. To our knowledge, this is the first study to illustrate the association of ABC in OS progression.

Although our study indicates the association of ABC with OS progression, there are some limitations in the current study. While the SaOS2/SaOS2-LM7 pair of cell lines showed definitive association of ABC with OS progression, our results with HOS/HOS-143B pair of cell lines presented with limited support for the association of ABC in OS progression. The sub-cellular localization studies that were carried out for HOS/HOS-143B showed mixed evidences for the association of nuclear ABC with OS progression. Among the two experimental techniques that were carried out to assess the sub-cellular localization of ABC, the western blot analysis of nuclear and cytoplasmic fractions showed inconclusive results; but, the immunofluorescence staining for ABC sub-cellular localization showed increased nuclear localization of ABC with OS progression. The inconclusive results from western blot analysis experiment was majorly due to the insufficient

number of repeats for the experiment. Therefore, it is required to carry out more replicates to arrive at a conclusion from this experiment. Despite the inconclusive western blot data for ABC in HOS/HOS-143B cell lines, the immunofluorescence imaging for ABC and its quantitative analysis using high content microscopy showed significant increase in the nuclear ABC with OS progression in HOS/HOS-143B cell lines. Hence, it still suggests the association of increased nuclear ABC with OS progression.

Cumulatively, the results from this study show that, while cellular levels and localization of ABC is associated with OS progression, total β-catenin itself is not associated with OS progression. Since ABC was differentially expressed in metastatic cell lines than parent cell lines, it might have a potential prognostic significance for OS. Further validation of the current findings in OS patient samples, might be useful for confirmation of the importance of ABC as a prognostic marker for OS. In our study, we showed the nuclear ABC level to be increased with OS progression. It is possible that the increased level of ABC in the nucleus likely promotes the transcription of downstream targets of Wnt signaling pathway, which subsequently promotes OS progression. Further studies need to be carried out to understand the mechanism by which this protein may promote OS progression.

	SaOS2 / SaOS2-LM7	HOS / HOS-143B
MMP Zymography (Metastatic potential)		
Cellular ABC		
Cellular β-catenin	No change	No change
Nuclear ABC		
Cytoplasmic ABC	No change	No change
Nuclear β-catenin	No change	No change
Cytoplasmic β-catenin	No change	No change

Figure 16: ***Summary of results in the current study.***

Chapter 5.0
Future directions

5.0. Future directions

5.1. Improvements for current study

The current study has provided supportive evidence that ABC could play a role in OS progression. However, additional improvements to the existing data would add strength to the study and provide more convincing conclusions.

5.1.1. Gelatin zymography with normalization to cell number

Currently, for the gelatin zymography experiments, conditioned media from the cell lines was collected at 80-90% confluence after same period of incubation in the serum free media. This is a widely followed method for gelatin zymography and it is therefore acceptable to carry out experiments in this manner. However, we are planning to add strength to this experiment by normalizing the MMP activity (densitometric value of the bands) to the number of cells that were present at the time of conditioned media recovery. Currently, we have carried out a few zymography experiments in which the number of cells were counted at the time of recovery of conditioned media (Figure A2). We are carrying out more replicates for this experiment.

5.1.2. High content microscopy experiment

The high content microscopy data has provided support for the increased nuclear ABC with OS progression in HOS/HOS-143B pair of cell lines. However, this experiment was not carried out for the other pair of cell lines; SaOS2/SaOS2-LM7. Hence, high content analysis for SaOS2/SaOS2-LM7 cell lines need to be carried out in future.

5.2. Prospective studies

5.2.1. Immunohistochemical staining for OS patient tissue samples

The results acquired from the experiments in our study using in-vitro model is indicative of the role of ABC in OS progression. Therefore, carrying out immunohistochemical staining for ABC in patient samples could impact the clinical relevance of our findings. In order to look at the clinical significance of ABC in OS progression, we plan on carrying out staining for ABC on a tumor microarray from Folio Biosciences (Catalog no. ARY-HH0085) that has 40 patient samples of OS

at different stages. Since, localization of ABC is of importance we plan to carry out 2 types of staining to detect the cellular localization; namely (i) immunohistochemical staining (IHC) and, (ii) immunofluorescence staining (IF). Currently, the optimizations for staining are in progress using normal bone tissues purchased from Folio Biosciences (See Appendix, A1.1. for staining protocol and Figures A3 and A4 for the preliminary results).

5.2.2. Identification of the role of ABC in OS progression

The current study has indicated that ABC plays a role in OS progression; therefore, one of our goals is to find how ABC might mediate the OS progression. To understand the mechanism by which ABC promotes OS progression, we plan to carry out over-expression studies with ABC. In pursuit of this, we have created an over-expression construct with a modified β-catenin gene in the backbone of pEGFP-C3 vector to generate ABC construct (See Appendix A1.2. for information on designing the construct). In addition to the functional ABC construct, we have a WT β-catenin construct that has been established in our lab previously. In order to compare the role of ABC and β-catenin in OS progression, we plan to transfect the parent OS cell lines with the following plasmids and compare the metastatic potential using functional assays that are described later in this section.

(i) p-EGFP-C3 vector control
(ii) p-EGFP-C3 WT β-catenin
(iii) p-EGFP-C3 ABC

A) Transfection of over-expression constructs

Currently we are optimizing a transfection protocol to achieve high transfection efficiency, to carry out the experiments for over-expression studies.

(i) Chemical transfection

Transfections using different chemical reagents like Fugene6, ExGen500 and Lipofectamine-2000 were tried on the HOS cell line. Transfection with Fugene6 was ineffective with poor transfection efficiency. Exgen500 and Lipofectamine-2000 showed few cells were transfected, but it was less than 10% transfection efficiency (Appendix A1.3 and Figure A5.1, A5.2, A5.3).

(ii) Transfection using electroporation

Electroporation was used as an alternate approach for transfection. We carried out an electroporation experiment for p-EGFP-C3-ABC at low capacitance and high voltage (See (Appendix A1.3. for electroporation conditions). However, the cells died after the electroporation. Therefore, it might be useful to try electroporating the cells at high capacitance and a range of low voltages from 200 V – 500 V as suggested by manufacturer of GenePulser (BioRad) for transfecting mammalian cells.

B) Quantitative RT-PCR (qRT-PCR) for Wnt downstream targets

If ABC plays a role in OS progression, one of the potential mechanisms for promoting metastasis would be through mediating the transcription of Wnt downstream targets. In order to confirm the transcriptional activity of ABC, a qRT-PCR for the downstream targets of Wnt that are known to be involved in OS metastasis could be carried out after over-expression experimental conditions. Some of the potential Wnt targets that are known to be involved in OS progression are VEGF-A, MMP2, MMP9, RANKL and OPG.

C) Functional assays

If ABC over-expression increases the mRNA levels of the downstream targets like VEGFA and MMP, the functional relevance of ABC could be understood by carrying out studies such as: (i) angiogenesis formation assay (152) (ii) migration assay and (iii) invasion assay. With ABC over-expression it would be expected to have more angiogenesis and migratory potential.

Chapter 6.0
Bibliography

6.0. Bibliography

1. Marieb EN. Human anatomy and physiology. New York: Pearson Education; 2004. 183-206 p.
2. Saladin KS. Anatomy & physiology : the unity of form and function. Seventh ed. New York: McGraw-Hill Education; 2015. 203-24 p.
3. Dwek JR. The periosteum: what is it, where is it, and what mimics it in its absence? Skeletal radiology. 2010;39(4):319-23.
4. Raggatt LJ, Partridge NC. Cellular and molecular mechanisms of bone remodeling. J Biol Chem. 2010;285(33):25103-8.
5. Florencio-Silva R, Sasso GR, Sasso-Cerri E, Simoes MJ, Cerri PS. Biology of Bone Tissue: Structure, Function, and Factors That Influence Bone Cells. BioMed research international. 2015;2015:421746.
6. Teitelbaum SL. Bone Resorption by Osteoclasts. Science. 2000;289(5484):1504-8.
7. Sims NA, Gooi JH. Bone remodeling: Multiple cellular interactions required for coupling of bone formation and resorption. Seminars in cell & developmental biology. 2008;19(5):444-51.
8. Phan TC, Xu J, Zheng MH. Interaction between osteoblast and osteoclast: impact in bone disease. Histology and histopathology. 2004;19(4):1325-44.
9. Prideaux M, Findlay DM, Atkins GJ. Osteocytes: The master cells in bone remodelling. Current opinion in pharmacology. 2016;28:24-30.
10. Li Y, Toraldo G, Li A, Yang X, Zhang H, Qian WP, et al. B cells and T cells are critical for the preservation of bone homeostasis and attainment of peak bone mass in vivo. Blood. 2007;109(9):3839-48.
11. Lorenzo J, Horowitz M, Choi Y. Osteoimmunology: interactions of the bone and immune system. Endocrine reviews. 2008;29(4):403-40.
12. Hauge EM, Qvesel D, Eriksen EF, Mosekilde L, Melsen F. Cancellous bone remodeling occurs in specialized compartments lined by cells expressing osteoblastic markers. Journal of bone and mineral research : the official journal of the American Society for Bone and Mineral Research. 2001;16(9):1575-82.
13. Heino TJ, Hentunen TA, Vaananen HK. Osteocytes inhibit osteoclastic bone resorption through transforming growth factor-beta: enhancement by estrogen. J Cell Biochem. 2002;85(1):185-97.
14. Aguirre JI, Plotkin LI, Stewart SA, Weinstein RS, Parfitt AM, Manolagas SC, et al. Osteocyte apoptosis is induced by weightlessness in mice and precedes osteoclast recruitment and bone loss. Journal

of bone and mineral research : the official journal of the American Society for Bone and Mineral Research. 2006;21(4):605-15.

15. Swarthout JT, D'Alonzo RC, Selvamurugan N, Partridge NC. Parathyroid hormone-dependent signaling pathways regulating genes in bone cells. Gene. 2002;282(1-2):1-17.

16. Li X, Qin L, Bergenstock M, Bevelock LM, Novack DV, Partridge NC. Parathyroid hormone stimulates osteoblastic expression of MCP-1 to recruit and increase the fusion of pre/osteoclasts. J Biol Chem. 2007;282(45):33098-106.

17. Ma YL, Cain RL, Halladay DL, Yang X, Zeng Q, Miles RR, et al. Catabolic effects of continuous human PTH (1--38) in vivo is associated with sustained stimulation of RANKL and inhibition of osteoprotegerin and gene-associated bone formation. Endocrinology. 2001;142(9):4047-54.

18. Yang CM, Chien CS, Yao CC, Hsiao LD, Huang YC, Wu CB. Mechanical strain induces collagenase-3 (MMP-13) expression in MC3T3-E1 osteoblastic cells. J Biol Chem. 2004;279(21):22158-65.

19. Pederson L, Ruan M, Westendorf JJ, Khosla S, Oursler MJ. Regulation of bone formation by osteoclasts involves Wnt/BMP signaling and the chemokine sphingosine-1-phosphate. Proceedings of the National Academy of Sciences of the United States of America. 2008;105(52):20764-9.

20. Zhao C, Irie N, Takada Y, Shimoda K, Miyamoto T, Nishiwaki T, et al. Bidirectional ephrinB2-EphB4 signaling controls bone homeostasis. Cell metabolism. 2006;4(2):111-21.

21. Canadian-cancer-statistics-2013, Canadian Cancer Society, Statistics Canada.

22. Mitra D, Shaw AK, Hutchings K. Trends in incidence of childhood cancer in Canada, 1992-2006. Chronic diseases and injuries in Canada. 2012;32(3):131-9.

23. Longhi A, Errani C, De Paolis M, Mercuri M, Bacci G. Primary bone osteosarcoma in the pediatric age: state of the art. Cancer treatment reviews. 2006;32(6):423-36.

24. Mirabello L, Troisi RJ, Savage SA. International osteosarcoma incidence patterns in children and adolescents, middle ages and elderly persons. International journal of cancer Journal international du cancer. 2009;125(1):229-34.

25. Ottaviani G, Jaffe N. The epidemiology of osteosarcoma. Cancer treatment and research. 2009;152:3-13.

26. Picci P. Osteosarcoma (osteogenic sarcoma). Orphanet journal of rare diseases. 2007;2:6.

27. Negrini S, Gorgoulis VG, Halazonetis TD. Genomic instability--an evolving hallmark of cancer. Nature reviews Molecular cell biology. 2010;11(3):220-8.

28. Miller CW, Aslo A, Won A, Tan M, Lampkin B, Koeffler HP. Alterations of the p53, Rb and MDM2 genes in osteosarcoma. Journal of cancer research and clinical oncology. 1996;122(9):559-65.

29. Ragazzini P, Gamberi G, Benassi MS, Orlando C, Sestini R, Ferrari C, et al. Analysis of SAS gene and CDK4 and MDM2 proteins in low-grade osteosarcoma. Cancer detection and prevention. 1999;23(2):129-36.

30. Scholz RB, Kabisch H, Weber B, Roser K, Delling G, Winkler K. Studies of the RB1 gene and the p53 gene in human osteosarcomas. Pediatric hematology and oncology. 1992;9(2):125-37.

31. Gokgoz N, Wunder JS, Mousses S, Eskandarian S, Bell RS, Andrulis IL. Comparison of p53 mutations in patients with localized osteosarcoma and metastatic osteosarcoma. Cancer. 2001;92(8):2181-9.

32. Ladanyi M, Cha C, Lewis R, Jhanwar SC, Huvos AG, Healey JH. MDM2 gene amplification in metastatic osteosarcoma. Cancer Res. 1993;53(1):16-8.

33. Maire G, Yoshimoto M, Chilton-MacNeill S, Thorner PS, Zielenska M, Squire JA. Recurrent RECQL4 imbalance and increased gene expression levels are associated with structural chromosomal instability in sporadic osteosarcoma. Neoplasia. 2009;11(3):260-8, 3p following 8.

34. Martin JW, Squire JA, Zielenska M. The genetics of osteosarcoma. Sarcoma. 2012;2012:627254.

35. Moore DD, Luu HH. Osteosarcoma. Cancer treatment and research. 2014;162:65-92.

36. Longhi A, Barbieri E, Fabbri N, Macchiagodena M, Favale L, Lippo C, et al. Radiation-induced osteosarcoma arising 20 years after the treatment of Ewing's sarcoma. Tumori. 2003;89(5):569-72.

37. Mendoza SM, Konishi T, Miller CW. Integration of SV40 in human osteosarcoma DNA. Oncogene. 1998;17(19):2457-62.

38. Ta HT, Dass CR, Choong PF, Dunstan DE. Osteosarcoma treatment: state of the art. Cancer metastasis reviews. 2009;28(1-2):247-63.

39. Wittig JC, Bickels J, Priebat D, Jelinek J, Kellar-Graney K, Shmookler B, et al. Osteosarcoma: a multidisciplinary approach to diagnosis and treatment. American family physician. 2002;65(6):1123-32.

40. Klein MJ, Siegal GP. Osteosarcoma: anatomic and histologic variants. American journal of clinical pathology. 2006;125(4):555-81.

41. Edward F. McCarthy FJF. Pathology of Bone and Joint disorders. Second ed. United Kingdom: Cambridge University Press; 2015. 187 - 272 p.

42. Vigorita VJ. Orthopaedic Pathology. Second ed: Lippincott Williams & Wilkins; 2008.

43. Sangle NA, Layfield LJ. Telangiectatic osteosarcoma. Archives of pathology & laboratory medicine. 2012;136(5):572-6.

44. Nakajima H, Sim FH, Bond JR, Unni KK. Small cell osteosarcoma of bone. Review of 72 cases. Cancer. 1997;79(11):2095-106.

45. Hang JF, Chen PC. Parosteal osteosarcoma. Archives of pathology & laboratory medicine. 2014;138(5):694-9.

46. Liu XW, Zi Y, Xiang LB, Han TY. Periosteal osteosarcoma: a review of clinical evidence. International journal of clinical and experimental medicine. 2015;8(1):37-44.

47. Widhe B, Widhe T. Initial symptoms and clinical features in osteosarcoma and Ewing sarcoma. The Journal of bone and joint surgery American volume. 2000;82(5):667-74.

48. Bacci G, Ferrari S, Sangiorgi L, Picci P, Casadei R, Orlandi M, et al. Prognostic significance of serum lactate dehydrogenase in patients with osteosarcoma of the extremities. Journal of chemotherapy (Florence, Italy). 1994;6(3):204-10.

49. Bacci G, Longhi A, Ferrari S, Lari S, Manfrini M, Donati D, et al. Prognostic significance of serum alkaline phosphatase in osteosarcoma of the extremity treated with neoadjuvant chemotherapy: recent experience at Rizzoli Institute. Oncology reports. 2002;9(1):171-5.

50. Bacci G, Picci P, Ferrari S, Orlandi M, Ruggieri P, Casadei R, et al. Prognostic significance of serum alkaline phosphatase measurements in patients with osteosarcoma treated with adjuvant or neoadjuvant chemotherapy. Cancer. 1993;71(4):1224-30.

51. Kaste SC. Imaging pediatric bone sarcomas. Radiologic clinics of North America. 2011;49(4):749-65, vi-vii.

52. Lodwick GS. A probabilistic approach to the diagnosis of bone tumors. Radiologic clinics of North America. 1965;3(3):487-97.

53. Morley N, Omar I. Imaging evaluation of musculoskeletal tumors. Cancer treatment and research. 2014;162:9-29.

54. deSantos LA, Bernardino ME, Murray JA. Computed tomography in the evaluation of osteosarcoma: experience with 25 cases. AJR American journal of roentgenology. 1979;132(4):535-40.

55. Kayton ML, Huvos AG, Casher J, Abramson SJ, Rosen NS, Wexler LH, et al. Computed tomographic scan of the chest underestimates the number of metastatic lesions in osteosarcoma. Journal of pediatric surgery. 2006;41(1):200-6; discussion -6.

56. McCarville MB, Christie R, Daw NC, Spunt SL, Kaste SC. PET/CT in the evaluation of childhood sarcomas. AJR American journal of roentgenology. 2005;184(4):1293-304.

57. Jawad MU, Scully SP. In brief: classifications in brief: enneking classification: benign and malignant tumors of the musculoskeletal system. Clinical orthopaedics and related research. 2010;468(7):2000-2.

58. Messerschmitt PJ, Garcia RM, Abdul-Karim FW, Greenfield EM, Getty PJ. Osteosarcoma. The Journal of the American Academy of Orthopaedic Surgeons. 2009;17(8):515-27.

59. Bacci G, Ferrari S, Lari S, Mercuri M, Donati D, Longhi A, et al. Osteosarcoma of the limb. Amputation or limb salvage in patients treated by neoadjuvant chemotherapy. The Journal of bone and joint surgery British volume. 2002;84(1):88-92.

60. Simon MA, Aschliman MA, Thomas N, Mankin HJ. Limb-salvage treatment versus amputation for osteosarcoma of the distal end of the femur. The Journal of bone and joint surgery American volume. 1986;68(9):1331-7.

61. Rougraff BT, Simon MA, Kneisl JS, Greenberg DB, Mankin HJ. Limb salvage compared with amputation for osteosarcoma of the distal end of the femur. A long-term oncological, functional, and quality-of-life study. The Journal of bone and joint surgery American volume. 1994;76(5):649-56.

62. Grimer RJ, Taminiau AM, Cannon SR. Surgical outcomes in osteosarcoma. The Journal of bone and joint surgery British volume. 2002;84(3):395-400.

63. Jaffe N. Historical perspective on the introduction and use of chemotherapy for the treatment of osteosarcoma. Adv Exp Med Biol. 2014;804:1-30.

64. Finklestein JZ, Hittle RE, Hammond GD. Evaluation of a high dose cyclophosphamide regimen in childhood tumors. Cancer. 1969;23(5):1239-42.

65. Selawry OS, Holland JF, Wolman IJ. Effect of vincristine (NSC-67574) on malignant solid tumors in children. Cancer chemotherapy reports Part 1. 1968;52(4):497-500.

66. Jaffe N, Traggis D, Enriquez C. Evaluation of a combination of mitomycin C (NSC-26980), phenylalanine mustard (NSC-14210), and vincristine (NSC-67574) in the treatment of osteogenic sarcoma. Cancer chemotherapy reports Part 1. 1971;55(2):189-91.

67. Groesbeck HP, Cudmore JT. EVALUATION OF 5-FLUOROURACIL (5-FU) IN SURGICAL PRACTICE. The American surgeon. 1963;29:683-91.

68. Cores EP, Holland JF, Wang JJ, Sinks LF. Doxorubicin in disseminated osteosarcoma. Jama. 1972;221(10):1132-8.

69. Jaffe N. Progress report on high-dose methotrexate (NSC-740) with citrovorum rescue in the treatment of metastatic bone tumors. Cancer chemotherapy reports Part 1. 1974;58(2):275-80.

70. Pratt C, Shanks E, Hustu O, Rivera G, Smith J, Kumar AP. Adjuvant multiple drug chemotherapy for osteosarcoma of the extremity. Cancer. 1977;39(1):51-7.

71. Eilber F, Giuliano A, Eckardt J, Patterson K, Moseley S, Goodnight J. Adjuvant chemotherapy for osteosarcoma: a randomized prospective trial. Journal of clinical oncology : official journal of the American Society of Clinical Oncology. 1987;5(1):21-6.

72. Souhami RL, Craft AW, Van der Eijken JW, Nooij M, Spooner D, Bramwell VH, et al. Randomised trial of two regimens of chemotherapy in operable osteosarcoma: a study of the European Osteosarcoma Intergroup. Lancet (London, England). 1997;350(9082):911-7.

73. Eselgrim M, Grunert H, Kuhne T, Zoubek A, Kevric M, Burger H, et al. Dose intensity of chemotherapy for osteosarcoma and outcome in the Cooperative Osteosarcoma Study Group (COSS) trials. Pediatric blood & cancer. 2006;47(1):42-50.

74. Bacci G, Fabbri N, Balladelli A, Forni C, Palmerini E, Picci P. Treatment and prognosis for synchronous multifocal osteosarcoma in 42 patients. The Journal of bone and joint surgery British volume. 2006;88(8):1071-5.

75. Kager L, Zoubek A, Kastner U, Kempf-Bielack B, Potratz J, Kotz R, et al. Skip metastases in osteosarcoma: experience of the Cooperative Osteosarcoma Study Group. Journal of clinical oncology : official journal of the American Society of Clinical Oncology. 2006;24(10):1535-41.

76. Raymond AK, Chawla SP, Carrasco CH, Ayala AG, Fanning CV, Grice B, et al. Osteosarcoma chemotherapy effect: a prognostic factor. Seminars in diagnostic pathology. 1987;4(3):212-36.

77. Phillips TL, Sheline GE. Radiatio herapy of malignant bone tumors. Radiology. 1969;92(7):1537-45.

78. Franchi A, Arganini L, Baroni G, Calzolari A, Capanna R, Campanacci D, et al. Expression of transforming growth factor beta isoforms in osteosarcoma variants: association of TGF beta 1 with high-grade osteosarcomas. The Journal of pathology. 1998;185(3):284-9.

79. Burrow S, Andrulis IL, Pollak M, Bell RS. Expression of insulin-like growth factor receptor, IGF-1, and IGF-2 in primary and metastatic osteosarcoma. Journal of surgical oncology. 1998;69(1):21-7.

80. Kappel CC, Velez-Yanguas MC, Hirschfeld S, Helman LJ. Human osteosarcoma cell lines are dependent on insulin-like growth factor I for in vitro growth. Cancer Res. 1994;54(10):2803-7.

81. Wadayama B, Toguchida J, Shimizu T, Ishizaki K, Sasaki MS, Kotoura Y, et al. Mutation spectrum of the retinoblastoma gene in osteosarcomas. Cancer Res. 1994;54(11):3042-8.

82. Wu JX, Carpenter PM, Gresens C, Keh R, Niman H, Morris JW, et al. The proto-oncogene c-fos is over-expressed in the majority of human osteosarcomas. Oncogene. 1990;5(7):989-1000.

83. Gamberi G, Benassi MS, Bohling T, Ragazzini P, Molendini L, Sollazzo MR, et al. C-myc and c-fos in human osteosarcoma: prognostic value of mRNA and protein expression. Oncology. 1998;55(6):556-63.

84. Zhao H, Wu Y, Chen Y, Liu H. Clinical significance of hypoxia-inducible factor 1 and VEGF-A in osteosarcoma. International journal of clinical oncology. 2015.

85. El Naggar A, Clarkson P, Zhang F, Mathers J, Tognon C, Sorensen PH. Expression and stability of hypoxia inducible factor 1alpha in osteosarcoma. Pediatric blood & cancer. 2012;59(7):1215-22.

86. Yang J, Yang D, Sun Y, Sun B, Wang G, Trent JC, et al. Genetic amplification of the vascular endothelial growth factor (VEGF) pathway genes, including VEGFA, in human osteosarcoma. Cancer. 2011;117(21):4925-38.

87. Kaya M, Wada T, Akatsuka T, Kawaguchi S, Nagoya S, Shindoh M, et al. Vascular endothelial growth factor expression in untreated osteosarcoma is predictive of pulmonary metastasis and poor prognosis. Clinical cancer research : an official journal of the American Association for Cancer Research. 2000;6(2):572-7.

88. Lammli J, Fan M, Rosenthal HG, Patni M, Rinehart E, Vergara G, et al. Expression of Vascular Endothelial Growth Factor correlates with the advance of clinical osteosarcoma. International orthopaedics. 2012;36(11):2307-13.

89. Bjornland K, Flatmark K, Pettersen S, Aaasen AO, Fodstad O, Maelandsmo GM. Matrix metalloproteinases participate in osteosarcoma invasion. The Journal of surgical research. 2005;127(2):151-6.

90. Wen X, Liu H, Yu K, Liu Y. Matrix metalloproteinase 2 expression and survival of patients with osteosarcoma: a meta-analysis. Tumour biology : the journal of the International Society for Oncodevelopmental Biology and Medicine. 2014;35(1):845-8.

91. Wang J, Shi Q, Yuan TX, Song QL, Zhang Y, Wei Q, et al. Matrix metalloproteinase 9 (MMP-9) in osteosarcoma: review and meta-analysis. Clinica chimica acta; international journal of clinical chemistry. 2014;433:225-31.

92. Li H, Zhang K, Liu LH, Ouyang Y, Bu J, Guo HB, et al. A systematic review of matrix metalloproteinase 9 as a biomarker of survival in patients with osteosarcoma. Tumour biology : the journal of the International Society for Oncodevelopmental Biology and Medicine. 2014;35(6):5487-91.

93. Duffy MJ. The urokinase plasminogen activator system: role in malignancy. Current pharmaceutical design. 2004;10(1):39-49.

94. Dass CR, Nadesapillai AP, Robin D, Howard ML, Fisher JL, Zhou H, et al. Downregulation of uPAR confirms link in growth and metastasis of osteosarcoma. Clinical & experimental metastasis. 2005;22(8):643-52.

95. Fisher JL, Mackie PS, Howard ML, Zhou H, Choong PF. The expression of the urokinase plasminogen activator system in metastatic murine osteosarcoma: an in vivo mouse model. Clinical cancer research : an official journal of the American Association for Cancer Research. 2001;7(6):1654-60.

96. Paoli P, Giannoni E, Chiarugi P. Anoikis molecular pathways and its role in cancer progression. Biochimica et biophysica acta. 2013;1833(12):3481-98.

97. Vachon PH. Integrin signaling, cell survival, and anoikis: distinctions, differences, and differentiation. Journal of signal transduction. 2011;2011:738137.

98. Marco RA, Diaz-Montero CM, Wygant JN, Kleinerman ES, McIntyre BW. Alpha 4 integrin increases anoikis of human osteosarcoma cells. J Cell Biochem. 2003;88(5):1038-47.

99. Laverdiere C, Hoang BH, Yang R, Sowers R, Qin J, Meyers PA, et al. Messenger RNA expression levels of CXCR4 correlate with metastatic behavior and outcome in patients with osteosarcoma. Clinical cancer research : an official journal of the American Association for Cancer Research. 2005;11(7):2561-7.

100. Kim SY, Lee CH, Midura BV, Yeung C, Mendoza A, Hong SH, et al. Inhibition of the CXCR4/CXCL12 chemokine pathway reduces the development of murine pulmonary metastases. Clinical & experimental metastasis. 2008;25(3):201-11.

101. Weng WH, Ahlen J, Astrom K, Lui WO, Larsson C. Prognostic impact of immunohistochemical expression of ezrin in highly malignant soft tissue sarcomas. Clinical cancer research : an official journal of the American Association for Cancer Research. 2005;11(17):6198-204.

102. Park HR, Jung WW, Bacchini P, Bertoni F, Kim YW, Park YK. Ezrin in osteosarcoma: comparison between conventional high-grade and central low-grade osteosarcoma. Pathology, research and practice. 2006;202(7):509-15.

103. Ogino W, Takeshima Y, Mori T, Yanai T, Hayakawa A, Akisue T, et al. High level of ezrin mRNA expression in an osteosarcoma biopsy sample with lung metastasis. Journal of pediatric hematology/oncology. 2007;29(7):435-9.

104. Ferrari S, Zanella L, Alberghini M, Palmerini E, Staals E, Bacchini P. Prognostic significance of immunohistochemical expression of ezrin in non-metastatic high-grade osteosarcoma. Pediatric blood & cancer. 2008;50(4):752-6.

105. Khanna C, Wan X, Bose S, Cassaday R, Olomu O, Mendoza A, et al. The membrane-cytoskeleton linker ezrin is necessary for osteosarcoma metastasis. Nature medicine. 2004;10(2):182-6.

106. Baldini N, Scotlandi K, Barbanti-Brodano G, Manara MC, Maurici D, Bacci G, et al. Expression of P-glycoprotein in high-grade osteosarcomas in relation to clinical outcome. The New England journal of medicine. 1995;333(21):1380-5.

107. Kinpara K, Mogi M, Kuzushima M, Togari A. Osteoclast differentiation factor in human osteosarcoma cell line. Journal of immunoassay. 2000;21(4):327-40.

108. Lee JA, Jung JS, Kim DH, Lim JS, Kim MS, Kong CB, et al. RANKL expression is related to treatment outcome of patients with localized, high-grade osteosarcoma. Pediatric blood & cancer. 2011;56(5):738-43.

109. Akiyama T, Dass CR, Choong PF. Novel therapeutic strategy for osteosarcoma targeting osteoclast differentiation, bone-resorbing activity, and apoptosis pathway. Molecular cancer therapeutics. 2008;7(11):3461-9.

110. Yao D, Cai GH, Chen J, Ling R, Wu SX, Li YP. Prognostic value of p53 alterations in human osteosarcoma: a meta analysis. International journal of clinical and experimental pathology. 2014;7(10):6725-33.

111. Nedelcu T, Kubista B, Koller A, Sulzbacher I, Mosberger I, Arrich F, et al. Livin and Bcl-2 expression in high-grade osteosarcoma. Journal of cancer research and clinical oncology. 2008;134(2):237-44.

112. Trieb K, Lehner R, Stulnig T, Sulzbacher I, Shroyer KR. Survivin expression in human osteosarcoma is a marker for survival. European journal of surgical oncology : the journal of the European Society of Surgical Oncology and the British Association of Surgical Oncology. 2003;29(4):379-82.

113. Ma Q, Zhou Y, Ma B, Chen X, Wen Y, Liu Y, et al. The clinical value of CXCR4, HER2 and CD44 in human osteosarcoma: A pilot study. Oncology letters. 2012;3(4):797-801.

114. Polakis P. Wnt signaling in cancer. Cold Spring Harb Perspect Biol. 2012;4(5).

115. Jamieson C, Sharma M, Henderson BR. Targeting the beta-catenin nuclear transport pathway in cancer. Seminars in cancer biology. 2014;27:20-9.

116. Valenta T, Hausmann G, Basler K. The many faces and functions of beta-catenin. The EMBO journal. 2012;31(12):2714-36.

117. Saito-Diaz K, Chen TW, Wang X, Thorne CA, Wallace HA, Page-McCaw A, et al. The way Wnt works: components and mechanism. Growth factors. 2013;31(1):1-31.

118. Staal FJ, Noort Mv M, Strous GJ, Clevers HC. Wnt signals are transmitted through N-terminally dephosphorylated beta-catenin. EMBO reports. 2002;3(1):63-8.

119. Macsai CE, Foster BK, Xian CJ. Roles of Wnt signalling in bone growth, remodelling, skeletal disorders and fracture repair. Journal of cellular physiology. 2008;215(3):578-87.

120. Chen K, Fallen S, Abaan HO, Hayran M, Gonzalez C, Wodajo F, et al. Wnt10b induces chemotaxis of osteosarcoma and correlates with reduced survival. Pediatric blood & cancer. 2008;51(3):349-55.

121. Hoang BH, Kubo T, Healey JH, Sowers R, Mazza B, Yang R, et al. Expression of LDL receptor-related protein 5 (LRP5) as a novel marker for disease progression in high-grade osteosarcoma. International journal of cancer Journal international du cancer. 2004;109(1):106-11.

122. Guo Y, Zi X, Koontz Z, Kim A, Xie J, Gorlick R, et al. Blocking Wnt/LRP5 signaling by a soluble receptor modulates the epithelial to mesenchymal transition and suppresses met and metalloproteinases in osteosarcoma Saos-2 cells. Journal of Orthopaedic Research. 2007;25(7):964-71.

123. Guo Y, Rubin EM, Xie J, Zi X, Hoang BH. Dominant negative LRP5 decreases tumorigenicity and metastasis of osteosarcoma in an animal model. Clinical orthopaedics and related research. 2008;466(9):2039-45.

124. Kansara M, Tsang M, Kodjabachian L, Sims NA, Trivett MK, Ehrich M, et al. Wnt inhibitory factor 1 is epigenetically silenced in human osteosarcoma, and targeted disruption accelerates osteosarcomagenesis in mice. The Journal of clinical investigation. 2009;119(4):837-51.

125. Hoang BH, Kubo T, Healey JH, Yang R, Nathan SS, Kolb EA, et al. Dickkopf 3 inhibits invasion and motility of Saos-2 osteosarcoma cells by modulating the Wnt-beta-catenin pathway. Cancer Res. 2004;64(8):2734-9.

126. Lin CH, Guo Y, Ghaffar S, McQueen P, Pourmorady J, Christ A, et al. Dkk-3, a secreted wnt antagonist, suppresses tumorigenic potential and pulmonary metastasis in osteosarcoma. Sarcoma. 2013;2013:147541.

127. Lee N, Smolarz AJ, Olson S, David O, Reiser J, Kutner R, et al. A potential role for Dkk-1 in the pathogenesis of osteosarcoma predicts novel diagnostic and treatment strategies. Br J Cancer. 2007;97(11):1552-9.

128. Iwaya K, Ogawa H, Kuroda M, Izumi M, Ishida T, Mukai K. Cytoplasmic and/or nuclear staining of beta-catenin is associated with lung metastasis. Clinical & experimental metastasis. 2003;20(6):525-9.

129. Haydon RC, Deyrup A, Ishikawa A, Heck R, Jiang W, Zhou L, et al. Cytoplasmic and/or nuclear accumulation of the beta-catenin protein is a frequent event in human osteosarcoma. International journal of cancer Journal international du cancer. 2002;102(4):338-42.

130. Ng TL, Gown AM, Barry TS, Cheang MC, Chan AK, Turbin DA, et al. Nuclear beta-catenin in mesenchymal tumors. Modern pathology : an official journal of the United States and Canadian Academy of Pathology, Inc. 2005;18(1):68-74.

131. Cai Y, Mohseny AB, Karperien M, Hogendoorn PC, Zhou G, Cleton-Jansen AM. Inactive Wnt/beta-catenin pathway in conventional high-grade osteosarcoma. The Journal of pathology. 2010;220(1):24-33.

132. Jia SF, Worth LL, Kleinerman ES. A nude mouse model of human osteosarcoma lung metastases for evaluating new therapeutic strategies. Clinical & experimental metastasis. 1999;17(6):501-6.

133. Ek ET, Dass CR, Choong PF. Commonly used mouse models of osteosarcoma. Crit Rev Oncol Hematol. 2006;60(1):1-8.

134. Brinckerhoff CE, Matrisian LM. Matrix metalloproteinases: a tail of a frog that became a prince. Nature reviews Molecular cell biology. 2002;3(3):207-14.

135. Snoek-van Beurden PA, Von den Hoff JW. Zymographic techniques for the analysis of matrix metalloproteinases and their inhibitors. BioTechniques. 2005;38(1):73-83.

136. Yasko AW. Surgical management of primary osteosarcoma. Cancer treatment and research. 2009;152:125-45.

137. Ferrari S, Smeland S, Mercuri M, Bertoni F, Longhi A, Ruggieri P, et al. Neoadjuvant chemotherapy with high-dose Ifosfamide, high-dose methotrexate, cisplatin, and doxorubicin for patients with localized osteosarcoma of the extremity: a joint study by the Italian and Scandinavian Sarcoma Groups. Journal of clinical oncology : official journal of the American Society of Clinical Oncology. 2005;23(34):8845-52.

138. Bacci G, Ferrari S, Bertoni F, Ruggieri P, Picci P, Longhi A, et al. Long-term outcome for patients with nonmetastatic osteosarcoma of the extremity treated at the istituto ortopedico rizzoli according to the istituto ortopedico rizzoli/osteosarcoma-2 protocol: an updated report. Journal of clinical oncology : official journal of the American Society of Clinical Oncology. 2000;18(24):4016-27.

139. Gaffney R, Unni KK, Sim FH, Slezak JM, Esther RJ, Bolander ME. Follow-up study of long-term survivors of osteosarcoma in the prechemotherapy era. Human pathology. 2006;37(8):1009-14.

140. Foukas AF, Deshmukh NS, Grimer RJ, Mangham DC, Mangos EG, Taylor S. Stage-IIB osteosarcomas around the knee. A study of MMP-9 in surviving tumour cells. The Journal of bone and joint surgery British volume. 2002;84(5):706-11.

141. Yonemoto T, Tatezaki S, Ishii T, Satoh T, Kimura H, Iwai N. Prognosis of osteosarcoma with pulmonary metastases at initial presentation is not dismal. Clinical orthopaedics and related research. 1998(349):194-9.

142. Bieling P, Rehan N, Winkler P, Helmke K, Maas R, Fuchs N, et al. Tumor size and prognosis in aggressively treated osteosarcoma. Journal of clinical oncology : official journal of the American Society of Clinical Oncology. 1996;14(3):848-58.

143. Grimer RJ, Sommerville S, Warnock D, Carter S, Tillman R, Abudu A, et al. Management and outcome after local recurrence of osteosarcoma. European journal of cancer (Oxford, England : 1990). 2005;41(4):578-83.

144. Bacci G, Donati D, Manfrini M, Forni C, Bertoni F, Gherlinzoni F, et al. [Local recurrence after surgical or surgical-chemotherapeutic treatment of osteosarcoma of the limbs. Incidence, risk factors and prognosis]. Minerva chirurgica. 1998;53(7-8):619-29.

145. Bacci G, Longhi A, Versari M, Mercuri M, Briccoli A, Picci P. Prognostic factors for osteosarcoma of the extremity treated with neoadjuvant chemotherapy: 15-year experience in 789 patients treated at a single institution. Cancer. 2006;106(5):1154-61.

146. Davis AM, Bell RS, Goodwin PJ. Prognostic factors in osteosarcoma: a critical review. Journal of clinical oncology : official journal of the American Society of Clinical Oncology. 1994;12(2):423-31.

147. Clark JC, Dass CR, Choong PF. A review of clinical and molecular prognostic factors in osteosarcoma. Journal of cancer research and clinical oncology. 2008;134(3):281-97.

148. Anninga JK, Gelderblom H, Fiocco M, Kroep JR, Taminiau AH, Hogendoorn PC, et al. Chemotherapeutic adjuvant treatment for osteosarcoma: where do we stand? European journal of cancer (Oxford, England : 1990). 2011;47(16):2431-45.

149. Mohseny AB, Machado I, Cai Y, Schaefer KL, Serra M, Hogendoorn PC, et al. Functional characterization of osteosarcoma cell lines provides representative models to study the human disease. Laboratory investigation; a journal of technical methods and pathology. 2011;91(8):1195-205.

150. Flores RJ, Li Y, Yu A, Shen J, Rao PH, Lau SS, et al. A systems biology approach reveals common metastatic pathways in osteosarcoma. BMC systems biology. 2012;6:50.

151. Kidani T, Nakamura A, Kamei S, Norimatsu Y, Miura H, Masuno H. Overexpression of cytoplasmic beta-catenin inhibits the metastasis of the murine osteosarcoma cell line LM8. Cancer cell international. 2014;14(1):31.

152. DeCicco-Skinner KL, Henry GH, Cataisson C, Tabib T, Gwilliam JC, Watson NJ, et al. Endothelial cell tube formation assay for the in vitro study of angiogenesis. Journal of visualized experiments : JoVE. 2014(91):e51312.

Appendix

Appendix – 1

Prospective studies – Materials and Methods

Appendix 1.0. Prospective studies: Materials and Methods

A1.1. Staining protocol for tissue samples

Immunofluorescence staining

Slides were baked at 60ºC for two hours and deparaffinized with Xylene and ethanol in the following order: Xylene – 3 times for 10 minutes each, followed by series of 100%, 95%, 75%, 50% each for 2 minutes. Slides were then boiled in citrate buffer (pH 6.0) for 11 minutes for antigen retrieval and washed in PBS after cooling down the slides. The permeabilization of tissue was done at 0.1% TritonX-100 in PBS for 5 minutes and then blocked using 5% goat serum in 0.3% PBST for one hour. The slides were incubated in primary antibody, Anti-ABC (1:100) at 4 ºC overnight. After primary antibody incubation, slides were washed 3 times in PBS for 5 minutes each and incubated with secondary antibody Alexafluor-555 (1:500) containing DAP1 for 1 hour. The slides were then washed with PBS 3 times and mounted using mounting media.

Immuno-histochemical staining

Slides were baked at 60ºC for one hour and de-paraffinized with Xylene and ethanol in the following order: Xylene – 1 time for 10 minutes and 2 times for 2 minutes each, followed by series of 100%, 95%, 85%, 75%, 50% ethanol each for 2 minutes and rehydrated with water for 5 minutes. Slides were then boiled in citrate buffer (pH 6.0) for 20 minutes in a pressure cooker for antigen retrieval and washed in PBS for 3 times, after cooling down the slides. The slides were blocked using 5% goat serum in 0.2% PBST for 2 hours and incubated with primary antibody, Anti-ABC (1:100, 1:300. 1:500, 1:1000) at 4 ºC overnight. After primary antibody incubation, slides were washed 3 times in PBST for 5 minutes each and incubated with biotinylated secondary antibody (1:200) for 2 hours. The slides were then washed with PBS 3 times and peroxidase activity was quenched using 0.3% hydrogen peroxide for 30 minutes. The staining was developed using DAB substrate by incubating until brown color was observed and then mounted using mounting media.

A1.2. Design of ABC over-expression construct

Currently, there are no available over-expression construct for ABC. Therefore, we created an ABC over-expression construct. The differential characteristic between the WT β-catenin and ABC is the phosphorylation status of NTD. β-catenin has four sites for phosphorylation namely, S33, S37, T41 and S45 in the NTD, whereas ABC is de-phosphorylated at the S37 and T41 but phosphorylated at S33 and S45. This difference in phosphorylation status between β-catenin and ABC was the basis for our construction of the over-expression plasmid.

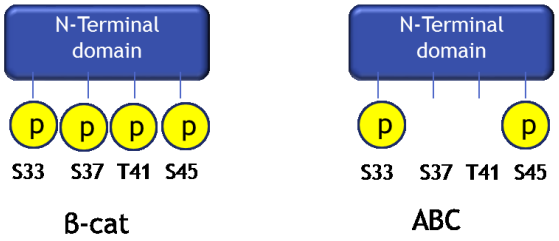

Figure A1: Phosphorylation status of β-catenin and ABC at NTD

We designed the ABC gene by replacing the S37 and T41 sites of WT β-catenin with Alanine (A). Replacement of S37 and T41 to alanine will prevent the sites from phosphorylation. In addition to this, the sites S33 and S45 were replaced with Aspartic acid (D). Aspartic acid has a chemical structure similar to phosphorylated Ser and thereby acts as a phosphomimetic. Hence, the replacement of S33 and S45 to aspartic acid makes these sites to be constitutively phosphorylated. Overall, the replacement of S33, S37, T41, S45 to D33, A37, A41, D45 might resemble ABC form.

The ABC gene was designed by modifying the codons of S33, S37, T41, S45 in WT β-catenin to codons coding for D33, A37, A41, D45. This modified gene was synthesized and cloned into pEGFP-C3 vector by GeneArt®. The sites of cloning for the synthesized ABC gene were Kpn1 and BamH1, the sites that were used for cloning WT β-catenin that has been previously designed in our lab. The vector designing was done and verified using a software called Vector NT1 with the guidance of Dr. Mary Hitt.

A1.3. Transfection optimization protocols for ABC transfection

1. Chemical transfection

The HOS cells were grown to 80% confluence overnight in pen-strep free media in a 6 well plate. Transfection was carried out using Lipofectamine-2000 reagent according to the manufacturer protocol. Briefly, two Eppendorf tubes were taken, with one containing plasmid DNA in 250ul OPTI-MEM media and another containing 10ul of Lipofectamine-2000 reagent in 250ul OPTI-MEM media. After 5 minutes of incubation, the Lipofectamine-2000/media mixture was added to the plasmid/media mixture and incubated for 20 minutes at room temperature. This complex is then added to the cells and incubated at 37ºC. After 24 hours, the cells were observed under a fluorescence microscope for detecting the GFP fluorescence. In the optimization protocol, different amounts of plasmid DNA were used (Figure A5).

2. Electroporation

Electroporation was carried out on 3x10^6 cells at constant capacitance (25uF) and various high voltage conditions. Following table shows the voltage settings that were used.

Condition no.	Voltage (kV)	Number pf pulses
1	1.0	1
2	1.0	2
3	1.0	3
4	1.5	1
5	1.5	2
6	2.0	1

Appendix – 2

Preliminary results

Appendix 2.0. Preliminary data

A2.1. Improvements for existing study: Gelatin zymography with cell count

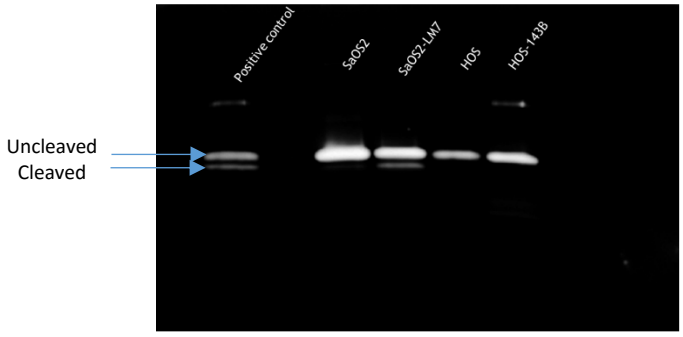

Cell lines	Cell count
SaOS2	1.5x10^5
SaOS2 - LM7	3.25x10^4
HOS	3.2x10^5
HOS-143B	4.5x10^5

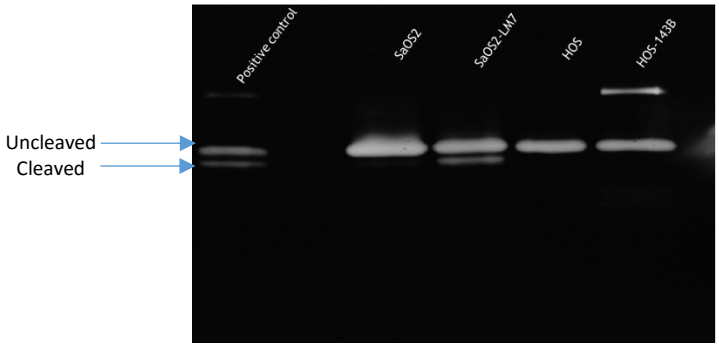

Cell lines	Cell count
SaOS2	2.6x10^5
SaOS2 - LM7	7x10^4
HOS	1.67x10^5
HOS-143B	4.5x10^5

Figure A2: ***Trial experiments for Gelatin zymography with cell count for normalization***. Two zymography experiments were carried out with counting the number of cells from which the conditioned media was concentrated. As seen in the columns, number of cells are lower for SaOS2-LM7 compared to SaOS2 but still has increased expression of cleaved form of MMP2. Similarly for HOS and HOS-143B, although there is a minor increase in the number of cells in HOS-143B, the MMP9 activity is significantly higher for HOS-143B with almost no activity in HOS.

A2.2. Prospective study: Optimization of IF and IHC staining

To optimize the IF staining protocol for OS tissue it is required to have a positive control (a tissue that stains positively for ABC). For this purpose, we optimized the staining protocol using EoE (Eosophagal Eosophagitis) tissue, which was previously shown to be positive for ABC staining in our laboratory. Further, we stained normal bone tissue for ABC using the same staining conditions that were used for EoE tissue. However, the staining was not efficient on bone tissue. The lack of staining in bone tissue might be due to the difference in the nature of EoE tissue in which the staining protocol was optimized. EoE tissue is of epithelial nature, whereas bone is mesenchymal. In order to improve the effectiveness of staining, the antigen retrieval time and primary antibody concentration were modified to stain bone tissue (Figure A3).

The IHC staining protocol was optimized on OS tumor sections. Different concentrations of primary antibody were used to optimize the best staining condition (Figure A4).

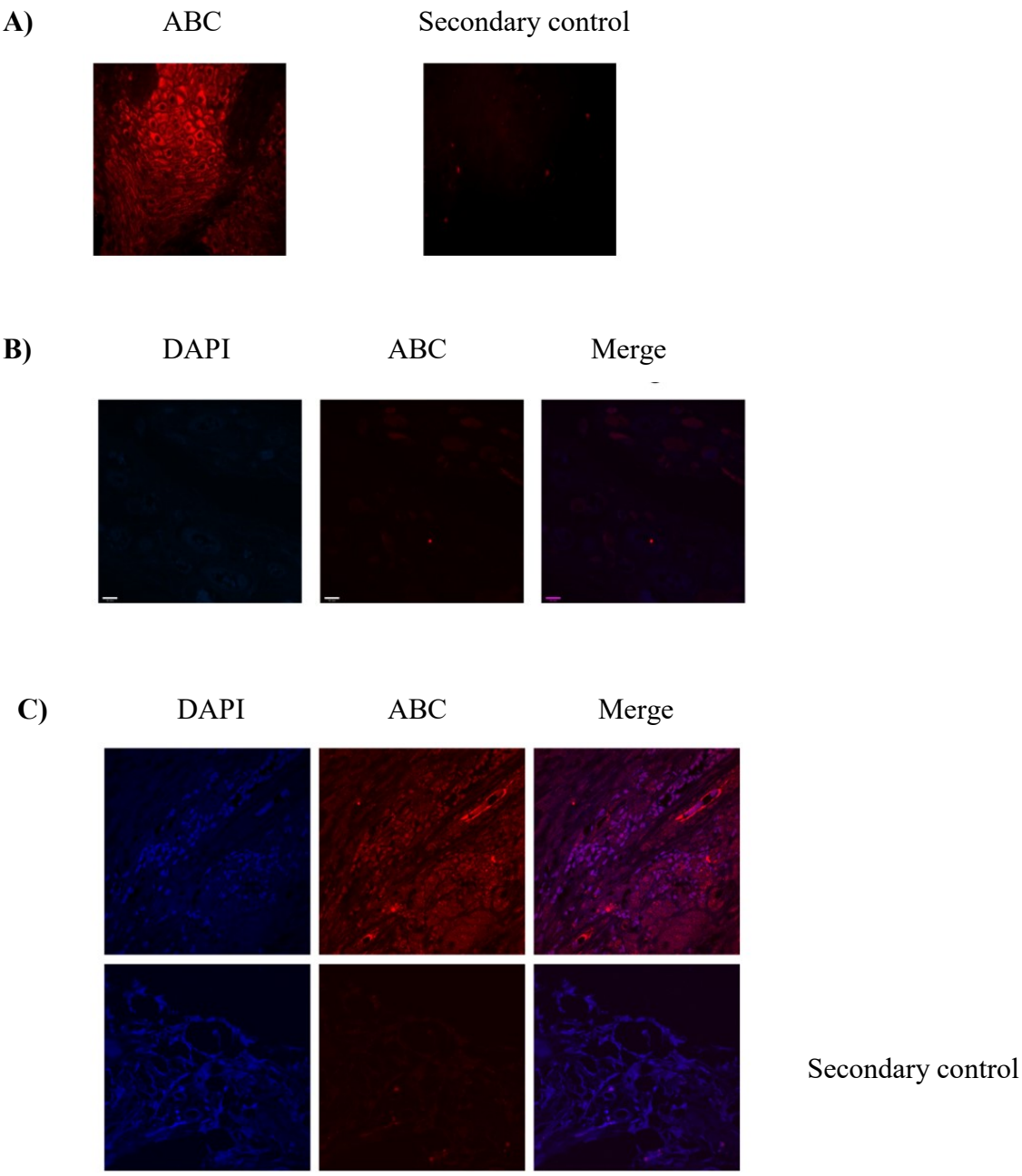

Figure A3: ***Optimization for IF staining***. A) ABC staining on EoE tissue with secondary antibody control. (ABC: 1 in 200 concentration) B) ABC staining on bone tissue at same staining conditions used for EoE (ABC: 1 in 200 concentration); Lack of ABC staining was observed C) ABC staining on normal bone tissue from human, with longer retrieval time and increased primary antibody concentration (ABC: 1in 100).

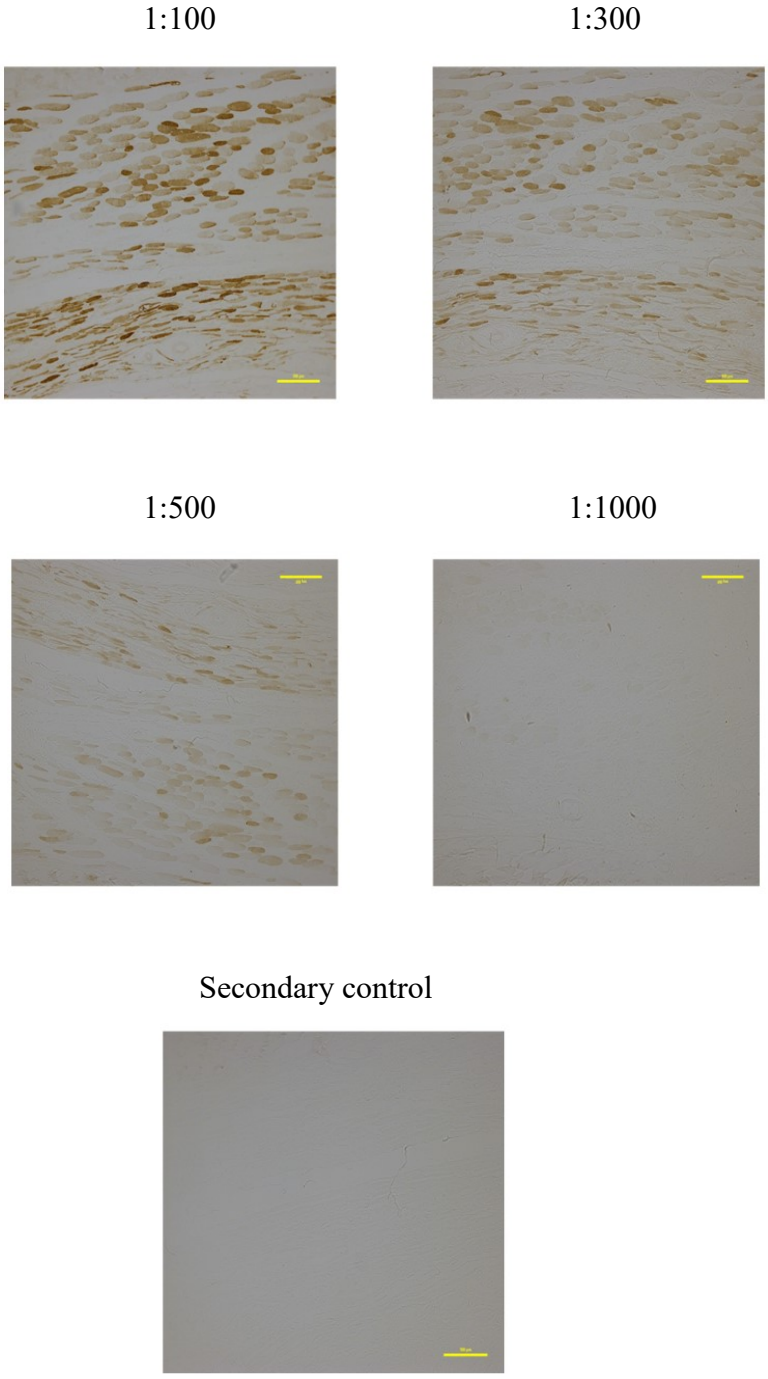

Credits: Staining was performed using the facility of Dr. David Eisenstat's lab with the guidance of Mr. Hunter Mccoll

Figure A4: ***Optimization for IHC staining.*** IHC for ABC on osteosarcoma single sections. Different primary antibody concentrations were used, 1:100, 1:300, 1:500, 1:1000. The dilution 1:100 and 1:300 produced good signal and therefore will be used in future staining.

A2.3. Prospective study: Optimization of transfection protocol for ABC and β-catenin constructs

A)

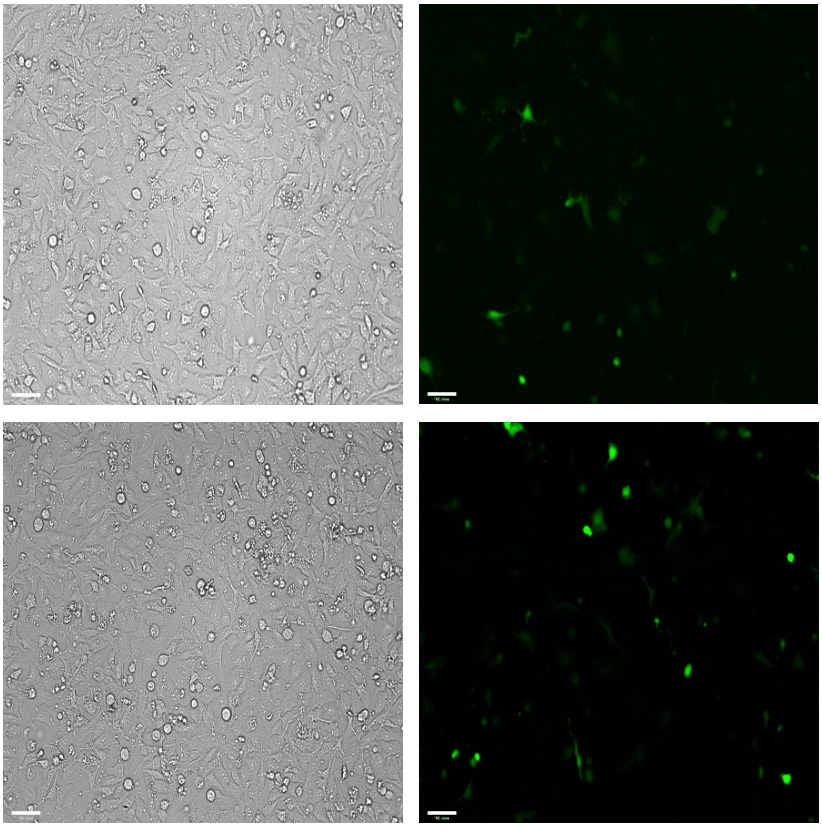

2ug p-EGFP plasmid

3ug p-EGFP plasmid

Figure A5.1. ***Transfection of pEGFP using Lipofectamine-2000***. 2 µg and 3 µg of p-EGFP plasmid DNA were transfected using Lipofectamine 2000 reagent and the transfection efficiency was determined after 24 hours.

B)

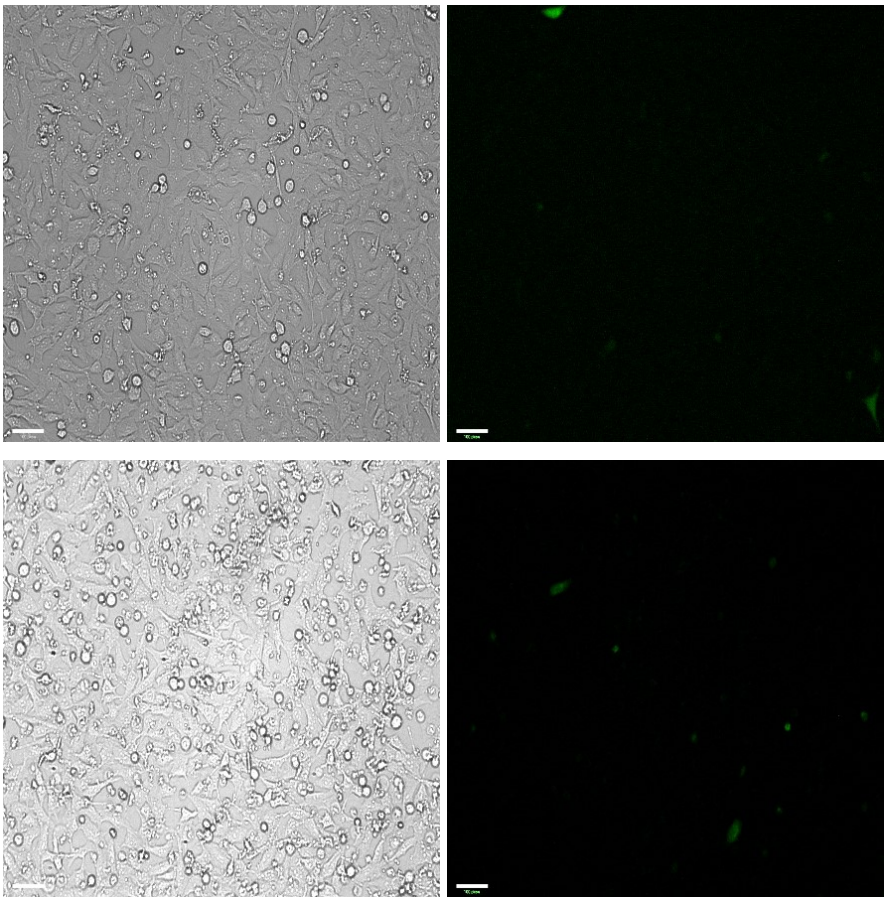

2ug pEGFP-β-catenin plasmid

3ug pEGFP- β-catenin plasmid

Figure A5.2. ***Transfection of pEGFP-β-catenin using Lipofectamine-2000***. 2 µg and 3 µg of p-EGFP-β-catenin plasmid DNA were transfected using Lipofectamine 2000 reagent and the transfection efficiency was determined after 24 hours.

C)

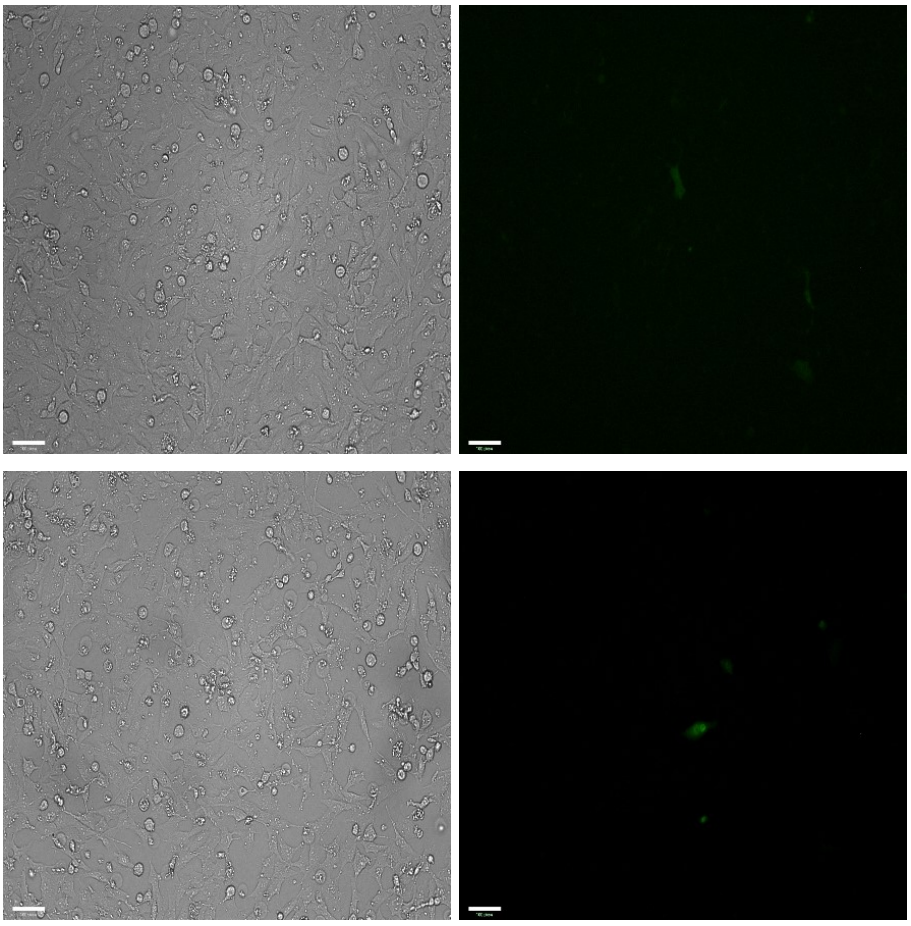

2ug pEGFP-ABC plasmid

3ug pEGFP-ABC plasmid

Figure A5.3. ***Transfection of pEGFP-ABC using Lipofectamine-2000***. 2 µg and 3 µg of p-EGFP-ABC plasmid DNA were transfected using Lipofectamine 2000 reagent and the transfection efficiency was determined after 24 hours.